

Accepted Manuscript

Seasonal phosphorus and carbon dynamics in a temperate shelf sea (Celtic Sea)

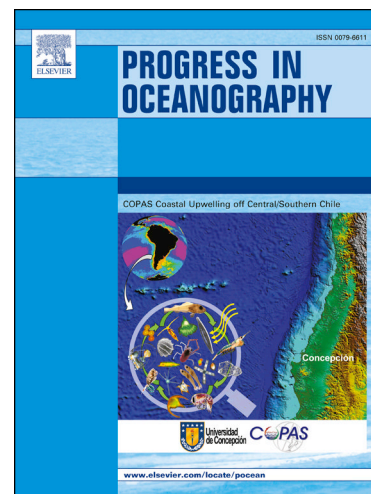
Alex J. Poulton, Clare E. Davis, Chris J. Daniels, Kyle M.J. Mayers, Carolyn Harris, Glen A. Tarran, Claire E. Widdicombe, E. Malcolm S. Woodward

PII: S0079-6611(17)30158-1

DOI: <https://doi.org/10.1016/j.pocean.2017.11.001>

Reference: PROOCE 1872

To appear in: *Progress in Oceanography*



Please cite this article as: Poulton, A.J., Davis, C.E., Daniels, C.J., Mayers, K.M.J., Harris, C., Tarran, G.A., Widdicombe, C.E., Woodward, E.M.S., Seasonal phosphorus and carbon dynamics in a temperate shelf sea (Celtic Sea), *Progress in Oceanography* (2017), doi: <https://doi.org/10.1016/j.pocean.2017.11.001>

This is a PDF file of an unedited manuscript that has been accepted for publication. As a service to our customers we are providing this early version of the manuscript. The manuscript will undergo copyediting, typesetting, and review of the resulting proof before it is published in its final form. Please note that during the production process errors may be discovered which could affect the content, and all legal disclaimers that apply to the journal pertain.

1 **Seasonal phosphorus and carbon dynamics in a temperate shelf sea (Celtic Sea)**

2

3 Alex J. Poulton^{1,†}, Clare E. Davis², Chris J. Daniels¹, Kyle M.J. Mayers³, Carolyn Harris⁴, Glen A.
4 Tarran⁴, Claire E. Widdicombe⁴, and E. Malcolm S. Woodward⁴

5

6 ¹ National Oceanography Centre, Waterfront Campus, Southampton, UK

7 ² Department of Earth, Ocean and Ecological Sciences, University of Liverpool, Liverpool, UK

8 ³ Ocean and Earth Science, University of Southampton, National Oceanography Centre
9 Southampton, Southampton, UK

10 ⁴ Plymouth Marine Laboratory, Prospect Place, The Hoe, Plymouth, UK

11

12 [†] Current address: The Lyell Centre, Heriot-Watt University, Edinburgh, UK

13 * Corresponding author.

14 Tel: +44 (0) 131 451 3891.

15 Email address: a.poulton@hw.ac.uk

16

17 **Highlights:**

- 18 • Seasonal uptake of phosphorus (P) and its dissolved organic release examined in Celtic Sea
- 19 • Uptake highest in spring bloom, with biomass-normalised affinity highest in summer
- 20 • Release high in November and late spring, with efficient P-retention and recycling in summer
- 21 • Strong phytoplankton influence on spring P-uptake, whilst bacteria influential in summer
- 22 • Relatively C-rich uptake in November and late April, P-rich in summer and early April

23 **Abstract**

24 The seasonal cycle of resource availability in shelf seas has a strong selective pressure on
25 phytoplankton diversity and the biogeochemical cycling of key elements, such as carbon (C) and
26 phosphorus (P). Shifts in carbon consumption relative to P availability, via changes in cellular
27 stoichiometry for example, can lead to an apparent 'excess' of carbon production. We made
28 measurements of inorganic P (P_i) uptake, in parallel to C-fixation, by plankton communities in the
29 Celtic Sea (NW European Shelf) in spring (April 2015), summer (July 2015) and autumn
30 (November 2014). Short-term (<8 h) P_i -uptake coupled with dissolved organic phosphorus (DOP)
31 release, in parallel to net (24 h) primary production (NPP), were all measured across an irradiance
32 gradient designed to typify vertically and seasonally varying light conditions. Rates of P_i -uptake
33 were highest during spring and lowest in the low light conditions of autumn, although biomass-
34 normalised P_i -uptake was highest in the summer. The release of DOP was highest in November and
35 declined to low levels in July, indicative of efficient utilization and recycling of the low levels of P_i
36 available. Examination of daily turnover times of the different particulate pools, including estimates
37 of phytoplankton and bacterial carbon, indicated a differing seasonal influence of autotrophs and
38 heterotrophs in P-dynamics, with summer conditions associated with a strong bacterial influence
39 and the early spring period with fast growing phytoplankton. These seasonal changes in autotrophic
40 and heterotrophic influence, coupled with changes in resource availability (P_i , light) resulted in
41 seasonal changes in the stoichiometry of NPP to daily P_i -uptake (C:P ratio); from relatively C-rich
42 uptake in November and late April, to P-rich uptake in early April and July. Overall, these results
43 highlight the seasonally varying influence of both autotrophic and heterotrophic components of
44 shelf sea ecosystems on the relative uptake of C and P.

45 **Keywords:** Phosphorus; Phosphate uptake; Dissolved organic Phosphorus; Stoichiometry.

46 **Regional index terms:** Celtic Sea; Northwest European Shelf.

47

48 1. Introduction

49 Phosphorus (P) is an essential nutrient for marine organisms, forming an important component of
50 various cellular constituents, including cell membranes and nucleic acids (RNA, DNA), and in the
51 transmission of chemical energy (Benitez-Nelson, 2000; Karl, 2000; Dyhrman et al., 2007). The
52 availability of P has an important role in controlling planktonic biomass and production and
53 community composition (Karl et al., 2001), with regionally low (pM) P concentrations limiting
54 biomass accumulation and biogeochemical processes (Moore et al., 2013). The biological cycling of
55 nutrients (P, N) are strongly coupled to the carbon (C) cycle via plankton biomass, resulting in
56 biological processes, such as photosynthesis and respiration, having a strong influence on
57 atmospheric CO₂ (Sterner and Elser, 2002; Arrigo, 2005).

58 The elemental stoichiometry (C:P, C:N) of plankton propagates through marine food webs to shape
59 ecosystem structure and function (Sterner and Elser, 2002; Elser et al., 2003), and hence plankton
60 provide an interface linking biogeochemical cycles, ecosystem dynamics and global climate
61 (Arrigo, 2005; Finkel et al., 2010). Understanding microbial elemental stoichiometry is important as
62 these relationships play major roles in coupled elemental cycles (Falkowski and Davis, 2004).

63 Planktonic micro-organisms, such as heterotrophic bacteria and phytoplankton, have rapid growth
64 rates and hence can exert a strong influence on the turnover of different C, N and P pools (Arrigo,
65 2005). Both phytoplankton and heterotrophic bacteria consume P, though the two have different
66 roles in the marine C-cycle as primary producers and remineralisers of organic material respectively
67 (Duhamel and Moutin, 2009), and they may compete strongly for available P when it is in short
68 supply (Thingstad et al., 1993, 1996).

69 In the marine environment, P is mainly found in dissolved inorganic and organic forms as well as in
70 particulate organic matter such as algal cells and detrital material. P is found in the form of
71 phosphate (P_i) with P predominately entering the ocean through rivers, and with the main losses
72 being through sedimentary processes (Benitez-Nelson, 2000; Karl, 2000; Dyhrman et al., 2002). The
73 production of DOP is via cellular exudation or lysis, as part of the production of dissolved organic
74 matter. Microbes directly incorporate P_i, though a small proportion of dissolved organic phosphorus
75 (DOP) may also be bioavailable and must be hydrolysed to be incorporated into the cell (Benitez-
76 Nelson, 2000).

77 In coastal waters, DOP concentrations range from 0 to 50% of the total P pool, while in the open
78 ocean it can be as high as 75% (Karl and Tien, 1992; Benitez-Nelson, 2000; Bjorkman et al., 2000;
79 Lønborg et al., 2009; Davis et al., 2014). Not all DOP is labile or bioavailable, with its availability
80 for biological uptake controlled by its chemical composition, and up to 50% of the DOP can be

81 refractory and inactive (Bjorkman et al., 2000; Bjorkman and Karl, 2003; Dyhrman et al., 2007;
82 Lønborg et al., 2009). The turnover rates of P within dissolved and particulate pools may be rapid
83 (from a few days to a couple of weeks), and vary over seasonal timescales, allowing low P to
84 support relatively high rates of primary production in coastal waters (Benitez-Nelson and Buesseler,
85 1999).

86 Redfield (e.g., Redfield et al., 1963) proposed that plankton and particulate material have a
87 relatively constrained elemental ratio (C:N:P) of 106:16:1, which matches closely with the average
88 ratio of dissolved inorganic N and P in seawater. These observations led to the paradigm that
89 plankton consume inorganic N and P in the same proportion as their availability, fixing them into
90 particulate organic material that is eventually decomposed, thus returning N and P back into their
91 inorganic forms (e.g., Redfield et al., 1963). This paradigm of elemental stoichiometry has been
92 used to link plankton production to the biogeochemical cycling of C, N and P. However, important
93 deviations from the canonical Redfield ratio may occur in the biochemical composition of marine
94 plankton (e.g., Geider and La Roche, 2002; Ho et al., 2003; Finkel et al., 2010), trophic interactions
95 (e.g., Sterner and Elser, 2002; Hessen et al., 2002, 2004) and biogeochemical processes (e.g.,
96 Arrigo, 2005; Bozec et al., 2006; Bauer et al., 2013).

97 As different cellular components, such as proteins and pigments, have their own stoichiometric
98 characteristics and represent significant amounts of the material in plankton cells, changes in their
99 relative proportions strongly influence bulk stoichiometry (Falkowski, 2000; Geider and La Roche,
100 2002). Under nutrient limited growth conditions plankton show increased cellular quotas of C,
101 suggesting increased uptake and storage of C-rich compounds (e.g., Geider and La Roche, 2002).
102 Rapid growth rates are predicted to lead to P-rich biomass as the cellular components required for
103 cell division have a high P-content (i.e., 'the growth rate hypothesis'; Sterner and Elser, 2002).
104 Variability in phytoplankton cellular composition (chlorophyll content, elemental stoichiometry)
105 also influences their quality as food items for higher trophic levels, and affects their growth rates
106 and trophic transfer efficiency (e.g., Hessen et al., 2002, 2004; Sterner and Elser, 2002).

107 The role of variable elemental stoichiometry is an important factor in determining the C-
108 sequestration efficiency of the Continental Shelf Pump (CSP) (Thomas et al., 2004, 2005; Bozec et
109 al., 2006). The CSP describes the process whereby CO₂, as dissolved inorganic carbon (DIC), is
110 transformed into particulate organic carbon (via photosynthesis) in the upper water column,
111 exported below the thermocline where it is remineralised back into DIC, and then this DIC is
112 advected into the adjacent open-ocean during winter time convective mixing (Thomas et al., 2004,
113 2005; Bozec et al., 2006). The efficiency of the CSP may be regulated by changing the ratio of
114 nutrient utilization for photosynthesis and production of particulate material, and by changing the

115 ratio of nutrient recycling and DIC remineralisation. For example, seasonal changes in DIC and
116 nutrient drawdown in the North Sea have shown that C-overconsumption occurs relative to nutrient
117 utilization, assuming Redfield stoichiometry (Toggweiler et al., 1993; Thomas et al., 2004, 2005;
118 Bozec et al., 2006; Kühn et al., 2010). Such C-overconsumption has been suggested to relate to
119 changes in plankton stoichiometry under seasonally varying resource availability (Toggweiler et al.,
120 1993; Thomas et al., 2004, 2005; Bozec et al., 2006; Kühn et al., 2010). Under nutrient limited
121 conditions plankton may show elevated, relative to the Redfield ratio, C-rich uptake and cellular
122 quotas, and release C-rich dissolved organic matter (e.g., Geider and La Roche, 2002; López-
123 Sandoval et al., 2011). However, direct measurements have yet to confirm whether C-
124 overconsumption in the CSP is a direct consequence of plankton stoichiometry or whether other
125 biogeochemical processes (e.g. nutrient recycling) are more influential on CSP efficiency. The
126 stoichiometry of primary production, nutrient uptake and recycling, trophic transfer and
127 decomposition, are all likely to influence the metabolic balance of shelf seas and the efficiency of
128 the CSP to varying degrees (Bauer et al., 2013).

129 Shelf seas represent less than 10% of the global ocean area, but are responsible for 10 to 30% of
130 primary production, as well as high proportions of global carbon sequestration (Joint et al., 2001;
131 Simpson and Sharples, 2012; Bauer et al., 2013). Hence, determining the processes that underpin
132 the magnitude and efficiency of the CSP is an important step in understanding how shelf seas attain
133 and maintain these roles with environmental variability. The aims of the present study were to: (1)
134 explore seasonal patterns in P_i -uptake and P-release (DOP production) relative to variability in
135 water-column structure, nutrient (N, P) availability, and plankton community composition; and (2)
136 examine the dynamics of P-biogeochemistry in terms of the turnover of different P pools and the
137 stoichiometry of P_i -uptake relative to C-fixation (net primary production, NPP). Overall, this paper
138 provides a better understanding of how the internal biogeochemical cycling of elements contribute
139 to the maintenance and efficiency of the CSP in the Celtic Sea. The specific hypotheses examined
140 are that: (a) the optimal growth conditions of the spring bloom lead to C-fixation and P_i -uptake at
141 ratios close to the Redfield ratio; whilst (b), departures from the Redfield ratio occur in response to
142 changes in resource (light, nutrient) availability.

143 **2. Methods**

144 **2.1. Sampling**

145 This study presents data collected from three cruises on-board the *RRS Discovery* to the Celtic Sea
146 over the period 2014 to 2015; the first in November 2014 (DY018: 9th November to 2nd
147 December), the second in spring 2015 (DY029: 1st April to 29th April), and the third and final

148 cruise in summer 2015 (DY033: 11th July to 2nd August). Each cruise focused on a different time-
149 period relevant to the ecosystem and biogeochemistry of the Celtic Sea, from the spring-bloom
150 (April) to summer stratified period (July), and onto the late autumn bloom and break down of
151 stratification (November). As part of this study, two sites were sampled for phosphate dynamics and
152 ancillary parameters, with the main site in the Central Celtic Sea (CCS; $\sim 49^{\circ}24' \text{ N}$, $8^{\circ}36' \text{ W}$; 150 m
153 water depth), and the second at the Shelf Break (CS2; $\sim 48^{\circ}34.26' \text{ W}$, $9^{\circ}30.58' \text{ W}$; 203 m water
154 depth) (Fig. 1). Over the three sampling periods these sites were repeatedly sampled, though CCS
155 was more frequently sampled ($n = 15$) than CS2 ($n = 6$).

156 Water samples were collected from six light depths in 20 L Niskin bottles on a CTD rosette sampler
157 deployed pre-dawn (02:00-06:00 h local time) at CCS and CS2. The light depths sampled were 60,
158 40, 20, 10, 5 and 1% of surface irradiance (Photosynthetically Active Radiation, PAR). Pre-dawn
159 sampling depths were determined by back calculation of the vertical attenuation coefficient of PAR
160 (K_d , m^{-1}), based on either: (a) an assumption that the base of the surface mixed layer (thermocline)
161 was at or close to the depth of the euphotic zone (i.e. 1% of surface irradiance) (November, April);
162 or (b) that the sub-surface chlorophyll-*a* maximum (SCM) occurred at or close to a depth of 5% of
163 surface irradiance (July) (Hickman et al., 2012).

164 Surface mixed layer (SML) depths were determined from processed CTD density data (J. Hopkins,
165 Liverpool, pers. comm.) through a two-step process. Firstly, SMLs were identified automatically by
166 applying a threshold for change in potential density with depth (an increase of either 0.02 kg m^{-3}
167 (November, July) or 0.01 kg m^{-3} (April) from the potential density at 10 m (or the nearest available
168 measurement)). Secondly, visual examination and confirmation for profiles that failed these criteria
169 or were close to the thresholds selected. Automatic detection of SML depths was successful at CCS,
170 though there were issues at CS2 due to internal wave breaking, and at CCS during April as the
171 stratification of the water-column evolved (J. Hopkins, Liverpool, pers. comm.). Identification of
172 the thermocline during the cruise was based on unprocessed CTD temperature data, while SML
173 identification was based on processed CTD density data. Hence, differences in SML and euphotic
174 zone depths during November and April are possible due to discrepancies in these data sources and
175 physical complexities of the water-column (especially during April and at the shelf break).

176 **2.2. Incubations**

177 Water samples for NPP, P_i -uptake and DOP production were all incubated in a purposely converted
178 and refitted commercial 20 foot ISO refrigeration shipping container (see Richier et al., 2014),
179 allowing incubation temperatures to be regulated at in situ values ($\pm 1\text{-}2^{\circ}\text{C}$). Each of the six
180 percentage light depths (60, 40, 20, 10, 5 and 1% of surface irradiance) had a dedicated incubation

181 chamber built, using blackout material to remove any light contamination between the different
182 light chambers. Irradiance was provided by one to three daylight simulation LED panels (Powerpax,
183 UK), each providing up to $100 \mu\text{mol quanta m}^{-2} \text{ s}^{-1}$, combined with different types of neutral density
184 filters (Lee FiltersTM, UK). The light-dark cycle was varied between different cruises to accurately
185 represent seasonal variability in photoperiods; 9 h in November, 14 h in April and 16 h in July.

186 To determine the seasonal range in incidental irradiance and allow representative daily light doses
187 to be determined for each light depth and each cruise, weekly average daily PAR levels (mol quanta
188 $\text{m}^2 \text{ d}^{-1}$) over a ten-year period (2003 to 2013) was determined from MODIS Aqua data (S. Henson,
189 Southampton, pers. comm.). Monthly averages over the ten years for incidental irradiance (E_0) for
190 each cruise period were then calculated for the position of the CCS site, giving values of 9.4 mol
191 $\text{quanta m}^{-2} \text{ d}^{-1}$ (November), $36.8 \text{ mol quanta m}^{-2} \text{ d}^{-1}$ (April), and $43.2 \text{ mol quanta m}^{-2} \text{ d}^{-1}$ (July).
192 Actual irradiance levels (E_0) during each cruise were measured by an on board *RRS Discovery* 2π
193 PAR irradiance sensor (Skye Instruments, SKE 510), with cruise averages (Table 1) showing
194 excellent agreement with long-term monthly averages.

195 Incidental irradiances for each month were corrected for reflective losses at the sea surface,
196 assuming an 8% loss (D. McKee, Strathclyde, pers. comm.) to give incidental irradiance (100%)
197 values and allow calculation of a light dose for each percentage irradiance chamber. Daily light
198 doses ($\text{mol quanta m}^{-2} \text{ d}^{-1}$) were reconstructed using a combination of LED panels and neutral
199 density filters, to achieve a target incidental irradiance per incubation chamber of 7 to $440 \mu\text{mol}$
200 $\text{quanta m}^{-2} \text{ s}^{-1}$, which were combined with the appropriate seasonal photoperiod to give a
201 representative seasonal daily light dose for each percentage light depth (see Supplementary Table
202 S1).

203 In summer, when strong vertical stratification occurred across the euphotic zone, the deeper light
204 depth (1%) samples were incubated in a Fytoscope FS130 laboratory incubator (Photon System
205 Instr., Czech Republic) at in situ temperatures ($\pm 1^\circ\text{C}$) and with a white LED light panel to replicate
206 the required light dose (see Supplementary Table S1). All light levels in the incubation chambers
207 and Fytoscope were checked with a 4π scalar PAR irradiance sensor (Biophysical Instruments,
208 QSL-2101).

209 Incubations for inorganic phosphate uptake and dissolved organic phosphorus release were short-
210 term ($<8 \text{ h}$; see below) and hence it is not appropriate to consider patterns in these rates against the
211 full daily light-dose experienced over the entire day-length. Rather, in this study, uptake and release
212 rates are presented (Figs. 2, 3, 4 and 6) against gradients in instantaneous irradiance (h^{-1}), but not

213 daily photon flux periods (d^{-1}). One important consequence of this is that seasonal changes in day-
214 length have no influence on the vertical patterns in uptake or release rates.

215 ***2.3. Inorganic Phosphate Uptake and Release of Dissolved Organic Phosphorus***

216 Hourly rates (dawn to midday, ~6-8 h) of inorganic phosphate uptake (P_i -uptake) were determined
217 following Rees et al. (1999), Björkman et al. (2000), and Reynolds et al. (2014). Water samples
218 from the six light depths were collected directly from the CTD under low-light conditions (pre-
219 dawn) into 500 mL brown NalgeneTM bottles which were returned to the on-board laboratory for
220 sub-sampling. Under low light conditions, sub-samples (3 light, 1 dark) were then dispensed into 70
221 mL polycarbonate bottles (Corning, Inc.) and each bottle spiked with either 111 to 222 kBq ^{33}P -
222 labelled orthophosphoric acid (PerkinElmer, Inc., specific activity 37 kBq $nmol^{-1}$) during April
223 2015 and November 2014, or 333 kBq ^{33}P -labelled orthophosphoric acid (Hartman Analytical
224 GmbH, specific activity 111 kBq $pmol^{-1}$) during July 2015. Use of these two isotopes ensured low
225 P_i addition and no enrichment of the ambient P_i pools; in the case of April and November the spike
226 addition resulted in ~3 to 6 nmol P (<3% of ambient P_i concentrations), and ~9 pmol in July (<1%
227 of ambient P_i concentrations). From one light bottle per light depth, three aliquots of 100 μ L were
228 then removed and placed into 7 mL glass scintillation vials to which 6 mL of Ultima GoldTM
229 (PerkinElmer, Inc.) liquid scintillation cocktail was added, and initial activities were counted at sea
230 on a Tri-Carb 3110TR scintillation counter. Triplicate light bottles and the single dark bottle were
231 then incubated in the controlled temperature (CT) incubators for 6 to 8 h at six irradiance levels (see
232 previous Section).

233 To determine P_i -uptake, incubations were terminated by filtration of each sample bottle (3 light, 1
234 dark) onto a 25 mm diameter 0.45 μ m polycarbonate NucleporeTM filter under gentle pressure.
235 Filtered samples were rinsed with unlabelled Whatman GF/F filtered seawater, air-dried and placed
236 in 7 mL glass scintillation vials and 6 mL of Ultima GoldTM (PerkinElmer, Inc.) liquid scintillation
237 cocktail added. Activity on the filters was then determined on a Tri-Carb 3100TR scintillation
238 counter, with P_i -uptake calculated following Björkman et al. (2000). P_i -uptake is represented both
239 on hourly time-scales (Fig. 3), averaged from the short-term (6-8 h) incubations, and scaled to a
240 daily (24 h) time-frame (Table 2) by multiplying hourly rates by 24 and assuming little or no
241 diurnal variability in P_i -uptake (see Discussion).

242 To determine the release of Dissolved Organic Phosphorus (DOP), at the end the incubation period
243 10 mL aliquots were removed from each of the four sample bottles (3 light, 1 dark) from three light
244 depths (60, 20 and 1% during November and April, 60, 5 and 1% during July). These aliquots were
245 gently filtered through 25 mm diameter 0.2 μ m Whatman NucleporeTM polycarbonate filters to

246 remove particulate material and the filtrate caught in 15 mL glass test tubes (10% Hydrochloric
247 acid-washed, Milli-Q-rinsed and oven-dried). Each 10 mL aliquot was then transferred to a plastic
248 15 mL centrifuge tube and 250 μ L of a 1 M sodium hydroxide solution (Sigma-Aldrich, UK) added
249 to precipitate out the dissolved P_i and leave the ^{33}P -labelled DOP (Karl and Tien, 1992; Thomson-
250 Bulldis and Karl, 1998; Björkman et al., 2000). Aliquots were shaken vigorously and centrifuged
251 for 1 h at 3500 rpm, with 1 mL of the supernatant removed from each, and placed in 7 mL glass
252 scintillation vials with 6 mL of Ultima GoldTM (PerkinElmer, Inc.) liquid scintillation cocktail. The
253 activity of the filtrate was then measured in a TriCarb 3100TR scintillation counter.

254 To estimate the proportion of DOP exuded relative to the phosphate (P_i) consumed, the gross rate of
255 P_i -uptake was estimated as the rate of P_i -uptake plus the rate of DOP production. Hence, we
256 calculated a percentage extracellular release for DOP as the fraction of total P_i -uptake (i.e., the sum
257 of P_i -uptake and DOP production) represented by DOP production alone, multiplied by 100. DOP
258 production is represented both on hourly time-scales (Fig. 4), averaged from the short-term (6-8 h)
259 incubations, and scaled to a daily (24 h) time-frame by multiplying hourly rates by 24 and assuming
260 little or no diurnal variability in DOP production.

261 The average relative standard deviation ($\text{RSD} = \text{standard deviation}/\text{Average} \times 100$) of triplicate P_i -
262 uptake measurements was 13% (range 2-49%) for November, 18% (3-67%) for April and 18% (1-
263 66%) for July. The average RSD of triplicate DOP production measurements was 31% (1-94%) for
264 November, 17% (1-39%) for April and 20% (2-53%) for July.

265 ***2.5. Particulate Organic Phosphorus and Dissolved Organic Phosphorus***

266 Water samples for determination of the concentrations of Particulate Organic Phosphorus (POP)
267 were collected from 6 to 8 depths (see Davis et al., this issue). Water samples (1 L) for POP
268 concentrations were filtered onto 25 mm Whatman GF/F (pre-combusted for 4 h at 450°C and
269 Hydrochloric acid-washed) glass-fibre filters (nominal pore size 0.7 μm) on a plastic filtering rig
270 under less than 12 kPa vacuum pressure. Filters were dried and POP concentrations determined
271 following Davis et al. (2014, this issue), with analysis in duplicate against certified reference
272 materials (CRM; SRM 1515 Apples Leaves, NIST) in triplicate with each sample extraction to
273 ensure analytical precision and accuracy of less than 2%. Sampling and storage bottles for POP and
274 DOP were pre-cleaned with 10% Hydrochloric acid and rinsed with Milli-Q before use. Samples for
275 DOP were pre-filtered through a combusted and acid-rinsed Whatman GF/F filter and stored in
276 HDPE bottles at -20°C before analysis. DOP concentrations were determined in triplicate by
277 measuring the difference in phosphate concentration before (total phosphate) and after (total
278 dissolved phosphate) UV oxidation.

279 Total dissolved phosphorus (TDP) was determined using the high temperature acid persulfate
280 technique as described in Lomas et al. (2010) with the following modifications. Standards were
281 made up in P-free artificial seawater using potassium monobasic phosphate (KHPO₄, Sigma
282 Aldrich). Samples and standards were autoclaved (121°C, 40 min) as 40 mL aliquots in tightly
283 sealed 50 mL glass Pyrex® bottles with Teflon® lined screw caps after addition of 5 mL potassium
284 persulfate solution (64 g/L). Following oxidation, samples were cooled overnight and then
285 precipitated using the magnesium induced co-precipitation (MAGIC) method (Karl and Tien, 1992)
286 by addition of 5 mL 1M sodium hydroxide solution (Sigma Aldrich). This step removed chloride
287 ions, which appeared to cause interference during DIP determination. Following centrifugation
288 (1000 x g, 60 min), the supernatant was discarded and the sample/standard pellet was completely
289 dissolved in 40 mL 0.1 M hydrochloric acid (Trace metal grade, Sigma Aldrich). Analytical blanks
290 were determined as described in Lomas et al. (2010).

291 Total dissolved phosphorus was determined in triplicate as dissolved inorganic phosphorus (DIP)
292 concentrations in the samples by the molybdenum blue method (Murphy and Riley, 1962) using a
293 Bran and Luebbe QuAAtro 5-channel auto-analyser (DIP detection limit 50 nM). At low DIP
294 concentrations (<100 nM), samples were reanalysed in triplicate 50 mL aliquots using the MAGIC
295 method (Karl and Tien, 1992) prior to DIP determination as above (detection limit 20 nM DIP).
296 Dissolved organic phosphorus (DOP) was quantified as the difference in DIP concentrations before
297 and after persulfate oxidation (i.e. DOP = TDP - DIP; DOP detection limit 40 nM).

298

299 **2.6. Nutrients and Chlorophyll-a**

300 Water samples for determination of nutrient concentrations (nitrate+nitrite, nitrite, phosphate, and
301 silicic acid) were collected directly from the CTD into aged, acid-washed and Milli-Q-rinsed 60 mL
302 HDPE Nalgene™ bottles. Clean sampling and handling techniques were employed during the
303 sampling and manipulations within the laboratory, and where possible carried out according to the
304 International GO-SHIP nutrient manual recommendations (Hydes et al., 2010). Nutrient samples
305 were all analysed on board the *RRS Discovery* using a Bran and Luebbe segmented flow
306 colorimetric auto-analyser using techniques described in Woodward and Rees (2001). Nutrient
307 reference materials (KANSO Japan) were run each day to check analyser performance and to
308 guarantee the quality control of the final reported data. The typical uncertainty of the analytical
309 results were between 2 to 3%, and the limits of detection for nitrate and phosphate was 0.02 µmol
310 L⁻¹, nitrite 0.01 µmol L⁻¹, whilst silicic acid was always higher than the limits of detection. Further
311 details of the nutrient analysis and seasonal variability in nutrient inventories can be found in
312 Humphreys et al. (this issue).

313 Water samples (0.2-0.25 L) for chlorophyll-*a* extraction were filtered onto 25 mm diameter
314 Whatman GF/F or Fisherbrand MF300 glass fibre filters (effective pore sizes 0.7 μm) and extracted
315 in 6 to 10 mL 90% acetone (HPLC grade, Sigma-Aldrich, UK) at -4°C for 18 to 24 h (Poulton et al.,
316 2014). Fluorescence was measured on a Turner Designs Trilogy fluorometer using a non-
317 acidification module and calibrated with a solid standard and a pure chlorophyll-*a* standard (Sigma-
318 Aldrich, UK).

319 **2.7. Primary Production**

320 Daily rates (dawn to dawn, 24 h) of primary production (i.e. Net Primary Production (NPP))
321 included in this paper were determined following the methodology outlined by Mayers et al. (this
322 issue) and Poulton et al. (2014). Seawater samples were collected from the same six light depths as
323 for P_i -uptake (see Section 2.3), directly from 20 L Niskin bottles on the CTD rosette into 500 mL
324 brown NalgeneTM bottles (10% Hydrochloric acid-washed, Milli-Q-rinsed) and transferred under
325 low light conditions to the on-board laboratory. In the laboratory, four (3 light, 1 formalin-killed
326 blank) 70 mL polycarbonate (CorningTM) bottles were filled per light depth. Carbon-14 (^{14}C)
327 labelled sodium bicarbonate (1258-1628 kBq) was added to each bottle and then three of the bottles
328 were incubated at the relevant light level in the CT container for 24 h (see Section 2.2). The fourth
329 sample (formalin-blank) had 1 mL of borate buffered formaldehyde (~1% final concentration)
330 added and was incubated alongside the other samples to measure abiotic uptake.

331 Incubations were terminated by filtering onto 25 mm 0.45 μm Whatman NucleporeTM
332 polycarbonate filters, with extensive rinsing to remove any unfixed ^{14}C -labelled sodium bicarbonate
333 remaining on the filters. Organic (NPP) carbon fixation was determined using the micro-diffusion
334 technique (see Mayers et al., this issue) in 20 mL glass vials with 1 mL of 1% orthophosphoric acid
335 added to remove any ^{14}C -particulate inorganic carbon, and 10 to 15 mL of Ultima GoldTM
336 (PerkinElmer, Inc.) liquid scintillation cocktail added to each sample. The activity on the filters was
337 then determined on a Tri-Carb 3100TR liquid scintillation counter on-board. Spike activity was
338 checked by removal of triplicate 100 μL subsamples directly after spike addition and mixing with
339 200 μL of β -phenylethylamine (Sigma-Aldrich, UK) followed by Ultima GoldTM addition and
340 liquid scintillation counting. The average RSD of triplicate NPP measurements was 15% (2-44%)
341 for November, 14% (1-59%) for April and 11% (1-42%) for July. The formalin blank consistently
342 represented less than 2% of NPP rates (cruise averages: 2%, November; 2%, April; 1%, July).

343 **2.8. Phytoplankton and Bacterial Carbon**

344 Cell abundances for the major phytoplankton groups were analysed from each sampling depth
345 within the euphotic zone, through either flow cytometry (for *Synechococcus*, pico-eukaryotes, nano-

346 eukaryotes, coccolithophores, cryptophytes, and bacteria) or light microscopy (for diatoms and
347 autotrophic dinoflagellates). Samples for flow cytometry were collected in clean 250 mL
348 polycarbonate bottles and analysed using a Becton Dickinson FACSort instrument (Tarran et al.,
349 2006) while samples for light microscopy were collected in 250 mL brown glass bottles and
350 preserved in acidic Lugol's solution (2% final solution) until analysis under an Olympus DMI4000B
351 microscope (Widdicombe et al., 2010).

352 Cell abundances from flow cytometer counts were converted to biomass using literature values
353 (Tarran et al., 2006): specifically, 8.58 fmol C cell⁻¹ for *Synechococcus*, 2.7 fmol C cell⁻¹ for
354 *Prochlorococcus*, 36.67 fmol C cell⁻¹ for pico-eukaryotes, 0.76 pmol C cell⁻¹ for nano-eukaryotes,
355 1.08 pmol C cell⁻¹ for coccolithophores, and 1.97 pmol C cell⁻¹ for cryptophytes. Heterotrophic
356 bacteria counts were converted to biomass using values of 1.58 fmol C cell⁻¹ for 'High Nucleic
357 Acid'-containing cells and 0.91 fmol C cell⁻¹ for 'Low Nucleic Acid'-containing cells. Cellular
358 biomass for light microscope counted taxa (diatoms and autotrophic dinoflagellates), were
359 estimated from cell dimensions following Kovalala and Larrence (1966) on an individual species
360 basis. For the estimates of phytoplankton carbon used in this study, a geometric mean value for all
361 the species present in the Celtic Sea samples was used: specifically, 19.58 pmol C cell⁻¹ for diatoms
362 and 85.25 pmol C cell⁻¹ for autotrophic dinoflagellates.

363 3. Results

364 3.1. Seasonal changes in environmental conditions in the Celtic Sea

365 Clear seasonal variability (Table 1) at both study sites (CCS, CS2) was evident in terms of changes
366 in the depth and average temperature of the surface mixed layer (SML), as well as the surface
367 concentration of inorganic phosphate (P_i) and nitrate+nitrite (NO_x). The SML shallowed from ~50
368 m to ~20 to 30 m and warmed by ~6°C between April and July, while it was at its deepest (average
369 50 m) and at intermediate temperatures (12.8-13.9°C) in November (Table 1). Nutrient
370 concentrations (both P_i and NO_x) were highest in early April and declined into low nutrient (P_i
371 <100 nmol P L⁻¹; NO_x <20 nmol N L⁻¹) summer conditions in July (Table 1). Significant temporal
372 variability was also observed throughout April, with the SML shallowing (from 51 to 16 m) and
373 warming by ~1°C, accompanied by the drawdown of both P_i (~300 nmol P L⁻¹) and NO_x (5.5 μmol
374 N L⁻¹). The ratio of NO_x to P_i, expressed as the deficit of NO_x relative to that expected if the two
375 were in Redfield proportions (i.e. N* = NO_x - (16 x P_i); see Moore et al., 2009), showed that shelf
376 waters were almost always depleted (relative to the Redfield ratio) in terms of NO_x, with most N*
377 values well below zero across all three sampling periods (Table 1). In fact, the N* values per cruise
378 were very similar, with little seasonal variability, whereas the absolute N:P ratio (mol:mol) was low

379 in November and April (~8-12 and 3-12, respectively) and extremely low (<0.5) in July (data not
380 shown; see also Humphreys et al., this issue).

381 Seasonal patterns were also obvious in terms of incidental irradiance (E_0) and SML average
382 irradiance (\bar{E}_{SML}), with both increasing from November to April and July (Table 1). November had
383 noticeably lower irradiance levels relative to both April and July, with the latter two months having
384 very similar irradiance levels despite differences in day length and euphotic zone depths (Table 1).
385 Euphotic zone depths in November were similar to SML depths, whereas SML depths were
386 generally shallow than euphotic zone depths in late April and July. Increasing \bar{E}_{SML} in April, in
387 parallel with nutrient drawdown, was associated with a shallowing of the SML rather than
388 increasing E_0 , and highlights the role of water-column structure in spring bloom development
389 (Table 1).

390 Discrete measurements of P_i over the euphotic zone also showed clear seasonal variability between
391 the sampling periods (Fig. 2a), with vertical differences absent in November and April but clearly
392 present in July. Concentrations of P_i were highest in April (up to $500 \text{ nmol P L}^{-1}$), varying from
393 ~200 to $500 \text{ nmol P L}^{-1}$ over the month, and lowest (< $100 \text{ nmol P L}^{-1}$) in July, apart from at the base
394 of the euphotic zone (> $100\text{-}600 \text{ nmol P L}^{-1}$) associated with a nutricline (Fig. 2a) and a Sub-surface
395 Chl-*a* Maximum (SCM; Fig. 2b). Euphotic zone Chl-*a* concentrations were also uniform with
396 sampling depth in November and April, while a SCM was evident in July with deep Chl-*a*
397 concentrations ranging from ~0.5 to 2.25 mg m^{-3} (Fig. 2b). The highest Chl-*a* concentrations, and
398 greatest variability, were observed in April during the spring bloom, with Chl-*a* at depth ranging
399 from ~1 to 8 mg m^{-3} (Fig. 2b). A slight variation to this pattern in April was observed at the deepest
400 sampling depth where Chl-*a* concentrations were consistently low ($1\text{-}2 \text{ mg m}^{-3}$) and similar to
401 concentrations at depth in November (Fig. 2b).

402 In terms of DOP concentrations (Fig. 2c), average discrete depth measurements in the euphotic zone
403 were high and relatively similar in November (266 to $389 \text{ nmol P L}^{-1}$) and April (241 to 438 nmol P
404 L^{-1}), but slightly lower in July (169 to $271 \text{ nmol P L}^{-1}$). No distinct depth pattern was evident
405 between November, April or July, with upper euphotic zone measurements similar to those found at
406 the base of the euphotic zone. In contrast to DOP, POP concentrations showed a different temporal
407 pattern, with the highest (> 75 nmol P L^{-1}) concentrations in April rather than November or July
408 (< 75 nmol P L^{-1}), though this trend was most clearly seen in the upper sampling depths of the
409 euphotic zone (Fig. 2d). Average POP concentrations in April in the upper euphotic zone ranged
410 from 91 to $133 \text{ nmol P L}^{-1}$, with averages in November and July ranging from 28 to 46 nmol P L^{-1}
411 and 23 to 51 nmol P L^{-1} , respectively.

412 3.2. Vertical profiles of Phosphate uptake

413 Discrete measurements of P_i -uptake over the euphotic zone (Fig. 3a) also showed clear seasonal
414 differences, with rates in April ($>1.5 \text{ nmol P L}^{-1} \text{ d}^{-1}$) much higher than those in July ($<1.5 \text{ nmol P L}^{-1}$
415 d^{-1}) or November ($<0.4 \text{ nmol P L}^{-1} \text{ d}^{-1}$). Upper euphotic zone P_i -uptake rates ranged from 1.2 to
416 $5.1 \text{ nmol P L}^{-1} \text{ h}^{-1}$ in April, 0.5 to $2.1 \text{ nmol P L}^{-1} \text{ h}^{-1}$ in July and 0.2 to $0.4 \text{ nmol P L}^{-1} \text{ h}^{-1}$ in
417 November. Uptake of P_i across the incubation light gradients showed light-dependent variability in
418 both November and April, being highest at the higher irradiance levels and decreasing with
419 declining irradiance (Fig. 3a). In contrast, P_i -uptake in July showed no dependency on incubation
420 irradiance despite the absolute irradiance levels being identical to April, most likely due to limiting
421 P_i concentrations in July (Fig. 2a) and hence substrate rather than irradiance dependency.

422 The ratio of light P_i -uptake to dark P_i -uptake was most often greater than 1, especially at irradiance
423 levels greater than $\sim 0.4 \text{ mol quanta m}^{-2} \text{ h}^{-1}$ during all three sampling periods (Fig. 3b). Ratios of
424 light to dark P_i -uptake were only less than 1 at the very lowest irradiance levels ($<0.1 \text{ mol quanta m}^{-2}$
425 h^{-1}) in November and April, whereas ratios rarely fell below 1 (or 1.5) during July. Ratios near
426 unity for light to dark P_i -uptake highlight how there was very little difference between light and
427 dark P_i -uptake rates in November and April, whereas a difference was more noticeable in July (Fig.
428 3b). For example, overall there was a 24% difference in average light and dark P_i -uptake rates in
429 November (0.21 and $0.16 \text{ nmol P L}^{-1} \text{ h}^{-1}$, respectively), and a 40% difference in July (0.89 and 0.53
430 $\text{nmol P L}^{-1} \text{ h}^{-1}$, respectively).

431 3.3. Vertical profiles of DOP production

432 The short-term production of DOP also showed clear seasonal differences, with rates being low
433 ($<0.2 \text{ nmol P L}^{-1} \text{ h}^{-1}$) in both November and July and higher (and more variable) in April (often
434 $>0.5 \text{ nmol P L}^{-1} \text{ h}^{-1}$) (Fig. 4a). Production of DOP over the three sampling depths ranged from 0.07
435 to $0.39 \text{ nmol P L}^{-1} \text{ h}^{-1}$ in November, from 0.10 to $1.78 \text{ nmol P L}^{-1} \text{ h}^{-1}$ in April and from 0.02 to 0.24
436 $\text{nmol P L}^{-1} \text{ h}^{-1}$ in July. Hence, although DOP production was similar in November and July, it was
437 slightly lower in July than November, and in April it varied from levels seen in the other months to
438 values 5 to 7 times higher. In all three sampling periods, no variability in DOP production occurred
439 in association with changes in the incubation irradiances (Fig. 4a): light-availability had no obvious
440 influence on DOP production. Ratios of light to dark DOP production were mostly greater than 1
441 during all three sampling periods, with very few measurements showing ratios less than 1 (Fig. 4b).
442 Light to dark DOP production ratios also showed no obvious variability in association with
443 incubation irradiance.

444 Expressing DOP production as a fraction of total P_i -uptake (i.e. the sum of P_i -uptake and DOP
445 production) shows clear patterns with sampling period and incubation irradiance (Fig. 4d). In
446 November, the percentage extracellular release of DOP was consistently greater than 25% and
447 increases up to 73% with decreasing incubation irradiance. A similar pattern was observed in April,
448 although the levels of DOP release were slightly lower (down to 5-10% in some cases) (Fig. 4d). In
449 contrast, DOP release in July was much lower (<20%) at all incubation irradiances, and in some
450 cases DOP release in July was less than 5% of total P_i -uptake. Clearly, when P_i concentrations are
451 at their lowest in July (<100 nmol P L⁻¹; Fig. 2a), DOP extracellular release (Figs. 4a and 4d) was at
452 its lowest level, despite relatively high rates of P_i -uptake (Fig. 3a).

453 **3.4. Integrated euphotic zone inventories**

454 Nutrient concentrations and rates of P cycling were integrated across the euphotic layer for all 3
455 cruises (November, April and July), which we considered to roughly match the SML in November
456 and early April, and then constrain both the SML and thermocline (and SCM) in late April and July
457 (see Table 1). Rates of NPP, P_i -uptake and DOP release were scaled to daily integrals.

458 Euphotic zone integrals of Chl-*a* showed a clear seasonal progression of the phytoplankton
459 communities, with average Chl-*a* concentrations highest in April (37.8-152.6 mg m⁻²), intermediate
460 in November (37.4-70.8 mg m⁻²) and lowest in July (17.2-35.7 mg m⁻²). Within April, Chl-*a*
461 concentrations went from 49.6 mg m⁻² in early April to a peak value of 152.6 mg m⁻² in mid-April,
462 which then decreased again towards the end of the month (Table 2). The mid-April Chl-*a* peak was
463 associated with the spring bloom at the CCS site (Mayers et al., this issue) and discrete water-
464 column Chl-*a* concentrations were as high as 8 mg m⁻³ (Fig. 2b). Increasing Chl-*a* concentrations
465 throughout April were associated with a significant drawdown of P_i , as shown by declining P_i
466 integrals from a high of 18.3 mmol P m⁻² to values similar to those observed in November and July
467 (i.e. <10 mmol P m⁻²; Table 2). However, the depth distribution of P_i was drastically different
468 between these two months (Fig. 2a): in November, moderate P_i concentrations (175-225 nmol P L⁻¹)
469 occurred throughout the water-column, while in July P_i concentrations were extremely low (<100
470 nmol P L⁻¹) in the upper water-column and increased dramatically (up to 600 nmol P L⁻¹) in
471 association with the nutricline (and SCM). Despite the presence of a SCM in July (Fig. 2b), this
472 month had the lowest water-column inventories for Chl-*a* (Table 2).

473 As with Chl-*a* measurements, estimates of euphotic zone integrated phytoplankton biomass (C_{phyto}),
474 based on conversion of cell counts, showed clear seasonal progression from low values in
475 November and July to peak concentrations in April (Table 2). Generally, estimates of C_{phyto} were
476 over 100 mmol C m⁻² during April and less than 80 to 90 mmol C m⁻² during the other sampling

477 periods. Estimated integrated bacteria biomass (C_{bact}) showed a similar seasonal pattern to C_{phyto} ,
478 relatively low and similar during November and July (ranges 24-32 and 23-33 mmol C m^{-2} ,
479 respectively) and peaking during April (27-182 mmol C m^{-2}) (Table 2). April was also associated
480 with an increase over time at CCS from low C_{bact} ($\sim 50 \text{ mmol C m}^{-2}$) to high values around the peak
481 in Chl-*a* around the latter half of the month ($>140 \text{ mmol C m}^{-2}$). Ratios of C_{bact} to C_{phyto} (data not
482 shown) were on average 0.34 (range 0.31-0.36) in November and 0.25 in July (0.17-0.37), and
483 increased to an average of 0.48 (0.29-0.82) in April, again showing a temporal progression as the
484 spring bloom peaked and nutrients declined.

485 Integrated net primary production (NPP) mirrored the seasonal changes in Chl-*a* concentrations,
486 with rates low in November (average 32.4 $\text{mmol C m}^{-2} \text{ d}^{-1}$) and July (average 35.4 $\text{mmol C m}^{-2} \text{ d}^{-1}$),
487 and peaking in mid-April at $\sim 0.5 \text{ mol C m}^{-2} \text{ d}^{-1}$ (Table 2). As with Chl-*a*, April showed relatively
488 low rates of NPP ($<120 \text{ mmol C m}^{-2} \text{ d}^{-1}$) early in the month, a peak on the 15th April and a decline
489 to values roughly half of the peak (132-321 $\text{mmol C m}^{-2} \text{ d}^{-1}$) at the end of the month. Clearly, the
490 spring bloom in 2015 at CCS was associated with significant carbon fixation (see also Mayers et al.,
491 this issue). Normalising NPP to Chl-*a* concentrations shows a similar seasonal pattern in terms of
492 the NPP per unit of phytoplankton biomass (Table 2). Integrated Chl-*a* normalised NPP rates were
493 similar in November (average 0.7 $\text{gC (g Chl)}^{-1} \text{ h}^{-1}$) and July (average 1.1 $\text{gC (g Chl)}^{-1} \text{ h}^{-1}$), and
494 peaked in mid-April with maximum values of 3.0 $\text{gC (g Chl)}^{-1} \text{ h}^{-1}$ (average 2.0 $\text{gC (g Chl)}^{-1} \text{ h}^{-1}$)
495 (Table 2). Such Chl-*a* normalised NPP rates indicate that phytoplankton communities in November
496 and July were fixing (photosynthetically) around the same amount of C per gram of (Chl-*a*)
497 biomass, while the community in April fixed almost double the amount for the same level of (Chl-
498 *a*) biomass.

499 Euphotic zone integrals of POP showed a similar April peak to Chl-*a* and NPP, with the highest
500 values in April (range 1.0 to 3.5 mmol P m^{-2} , average 2.3 mmol P m^{-2}), and with lower and more
501 similar values in July (1.0-2.0 mmol P m^{-2}) and November (1.0-2.2 mmol P m^{-2}) (Table 2). Some of
502 the highest integrated POP values ($>3 \text{ mmol P m}^{-2}$) occurred in association with the high levels of
503 Chl-*a* and NPP in mid-April at CCS. In contrast to POP (Chl-*a* and NPP), water-column integrated
504 DOP concentrations showed a different seasonal pattern with values in November being the highest
505 (11-25 mmol P m^{-2}), and with lower values in April (6-13 mmol P m^{-2}) and July (3-10 mmol P m^{-2})
506 (Table 2; see also Davis et al., this issue). In both April and July, integrated DOP concentrations
507 were roughly equivalent to the size of the ambient P_i pool in the euphotic zone, while in November
508 DOP concentrations were slightly higher than P_i . Though significant P_i drawdown was seen during
509 April, there was no concurrent increase in the DOP pool, which only varied in size by ~ 6 to 7 mmol

510 $P\ m^{-2}$ relative to a clear P_i drawdown of $\sim 12\ mmol\ P\ m^{-2}$ and a ~ 2 to $3\ mmol\ P\ m^{-2}$ increase in POP
511 (Table 2).

512 The seasonal pattern of euphotic zone integrated P_i -uptake showed a peak in April (average 1.61
513 $mmol\ P\ m^{-2}\ d^{-1}$), with the July average roughly half of that in April ($0.84\ mmol\ P\ m^{-2}\ d^{-1}$) and the
514 lowest rates ($<0.30\ mmol\ P\ m^{-2}\ d^{-1}$) in November (Table 2). The highest rate of integrated P_i -
515 uptake occurred in mid-April ($2.08\ mmol\ P\ m^{-2}\ d^{-1}$) in association with the peak values of Chl-*a* and
516 NPP. However, unlike Chl-*a* and NPP, the P_i -uptake rates throughout April were much higher
517 (generally $>1.3\ mmol\ P\ m^{-2}\ d^{-1}$) than those measured during the other sampling periods (range 0.14 -
518 $0.30\ mmol\ P\ m^{-2}\ d^{-1}$ for November and 0.48 - $1.18\ mmol\ P\ m^{-2}\ d^{-1}$ for July). In the case of integrated
519 DOP production (Table 2), the highest values occurred in April (average $0.49\ mmol\ P\ m^{-2}\ d^{-1}$), with
520 values in November ~ 3 times higher (average $0.17\ mmol\ P\ m^{-2}\ d^{-1}$) than those in July (average 0.05
521 $mmol\ P\ m^{-2}\ d^{-1}$). This pattern contrasts to that of the integrated P_i -uptake, with the highest DOP
522 production ($>0.8\ mmol\ P\ m^{-2}\ d^{-1}$) occurring not in association with the peak in P_i -uptake, Chl-*a* or
523 NPP but rather 5 to 9 days later in April (Table 2). When integrated DOP production is expressed as
524 a fraction of total P_i -uptake (see Section 3.3) there are strong differences between the three
525 sampling periods (Table 2); DOP production represents (on average) a much higher fraction of total
526 P_i -uptake in November (41%) than in April (21%) or July (6%) (Table 2). The percentage
527 extracellular release of DOP was extremely low ($<5\%$) in some cases in early July, with the low
528 values ($<15\%$) seen in July only observed elsewhere during early April, well before the
529 development of the spring bloom and peak Chl-*a* around the 15th April.

530 4. Discussion

531 4.1. The dynamics of Phosphate uptake

532 The uptake of nutrients (N, P) and photosynthetic C-fixation, and the resulting stoichiometric
533 balance of cellular constituents vary on timescales from almost instantaneous to daily adjustments
534 (e.g., Geider and La Roche, 2002; Rees et al., 1999; Talmy et al., 2014; Lopez et al., 2016).
535 Ecological interactions also occur across various timescales, resulting in stoichiometric balances
536 that vary in time and space, with important implications for the biogeochemistry of marine
537 ecosystems (Sterner and Elser, 2002). Short-term measurements need to be scaled to the appropriate
538 integrated time- and depth-scales (e.g. daily, euphotic zone), and with clear perspectives on what is
539 (or is not) measured is required prior to examining system-scale biogeochemical processes.

540 The potentially rapid recycling of P leads to the requirement that uptake (and release) measurements
541 are considered over short-time periods, whereas photosynthetic C-fixation occurs throughout the
542 (seasonally variable) daylight period. Short-term P_i -uptake measurements are often scaled to a 24 h

543 period, with the inherent assumption that uptake rates are temporally invariable. To examine this,
544 we undertook two time-series incubations of P_i -uptake, with measurements every 4 h over a period
545 of 24 h (Fig. 5). One time-series incubation began at 6 am (local time) on the 17th July and the
546 second at 9 am (local time) on the 23rd July, with both experiments showing a steady increase in P_i -
547 uptake prior to sunset and then a slight decline during the night (Fig. 5a). Average P_i -uptake (\pm
548 S.D.) for these incubations was 0.72 ± 0.20 and 0.92 ± 0.22 $\text{nmol P L}^{-1} \text{ h}^{-1}$, respectively, which are
549 higher than the initial 4 h measurements (0.43 ± 0.06 and 0.67 ± 0.08 $\text{nmol P L}^{-1} \text{ h}^{-1}$, respectively).
550 If the initial measurements are scaled by 24 h, daily rates of 9.6 $\text{nmol P L}^{-1} \text{ d}^{-1}$ and 16.8 nmol P L^{-1}
551 d^{-1} are calculated, which are 26 to 47% less than the cumulative 24 h rates (Fig. 5b). These results
552 caution that short-term rates of P_i -uptake may vary during day- and night-time periods, and hence
553 scaling these initial rates may result in a significant underestimation of daily P_i -uptake.

554 However, these results should also be viewed cautiously, as they represent only two time-series of
555 P_i -uptake, when P_i concentrations were at their lowest seasonal level (Table 1). Further time-series
556 of P_i -uptake need to be considered in the context of diurnal changes in cellular metabolism, and
557 between different components of the plankton (bacteria, phytoplankton). Interpretation of diurnal
558 changes in P_i -uptake may also be complicated if, for example, P_i concentrations and biomass are not
559 constant in the incubations (neither of which were measured in our experiments). Though we
560 acknowledge that short-term P_i -uptake measurements may not simply scale with day length (Fig. 5),
561 to make our observations consistent with the existing literature (e.g., Reynolds et al., 2014) we have
562 retained simple scaling to day lengths. Furthermore, the focus of the present study was to examine
563 seasonal (inter-cruise) differences in P_i -uptake and such overestimates may be systematic for each
564 sampling period.

565 Both bacteria and phytoplankton are involved in P uptake in marine systems (Popendorf and
566 Duhamel, 2015), with phytoplankton P_i -uptake related to some extent by light availability whilst
567 bacterial uptake may be unrelated to light level. Across all three seasonal sampling periods, rates of
568 both P_i -uptake and DOP production in light-exposed (L) incubations were higher than those
569 incubated in the dark (D), with L:D ratios consistently greater than 1 (Figs. 3b and 4b). For P_i -
570 uptake, L:D ratios were greater than 1.5 at the highest incubation irradiances (>0.6 mol quanta m^{-2}
571 h^{-1}) in November and April, and across most of the light gradient in July. Light availability clearly
572 enhanced P_i -uptake, which may be analogous to the reduced rates of P_i -uptake during the night-time
573 time-series experiments (Fig. 5a).

574 In the case of DOP production, L:D ratios were also slightly higher than 1 during July, and in
575 general the L:D ratios were similar in magnitude and trend to those seen in P_i -uptake (Fig. 4b):
576 hence the irradiance-influence on P_i -uptake was mirrored in the subsequent release of DOP, though

577 the relative percentage extracellular release of DOP differed seasonally (Fig. 4d). Ratios of L:D P_i-
578 uptake in other studies have also been found to be greater than 1, for example in the North Atlantic
579 (Donald et al., 2001) and Pacific Ocean (Duhamel et al., 2012), although ratios closer to 1 have
580 been reported from the North Pacific subtropical gyre (Björkman et al. 2000). Variability in L:D
581 uptake ratios likely reflects the relative contribution of phytoplankton and bacteria, as well as
582 seasonal variability in substrate (P_i) availability and energetic (light, C) constraints on P_i-uptake and
583 cellular P-demands (Sterner and Elser, 2002; Björkman et al., 2000).

584 Competition between bacteria and phytoplankton for P is a strong driver of biogeochemistry in
585 marine ecosystems (Thingstad et al., 1993, 1996; Poppendorf and Duhamel, 2015). Previous studies
586 of planktonic P_i-uptake have shown differentiated bacterial and algal P-uptake using different pore-
587 sized filters, for example considering bacterial uptake as from cells less than 0.6 µm and algal
588 uptake from cells greater than 0.6 µm (e.g., Duhamel and Moutin, 2009). However, both bacterial
589 and algal cell sizes are variable with taxonomy and physiological status and may overlap in size-
590 distribution; for example, the cyanobacteria *Synechococcus*, which is numerically dominant in the
591 Celtic Sea in summer (Hickman et al., 2012), and ranges in cell size in association with growth rate
592 and nutrient conditions (Lopez et al., 2016). In this study, 0.45 µm filters were used to ensure that
593 P_i-uptake from *Synechococcus* was fully included in our measurements at the same time as (partly)
594 excluding the influence of heterotrophic bacteria.

595 To test this assumption, size-fractionation experiments were performed during summer with
596 samples size-fractionated (0.2, 0.45, 0.8 and 2 µm) post-incubation to determine the P_i-uptake by
597 different fractions (Supplementary Fig. S1). These experiments indicated that the 0.45 µm P_i-uptake
598 represented on average 55% (range 32-84%) of the total (0.2 µm) P_i-uptake, while the 0.8 µm
599 fraction represented 36% (19-42%), and the greater than 2 µm fraction 14% (10-19%). These
600 differential contributions are similar to those found by Duhamel and Moutin (2009) (~15-43% 0.2-
601 0.6 µm, ~20-75% 0.6-2 µm, ~10-50% >2 µm), implying that although the use of 0.45 µm filters
602 removed a proportion of bacterial P_i-uptake (0.2-0.45 µm), our measurements of P_i-uptake may not
603 be exclusively from phytoplankton and likely include some bacterial P_i-uptake. Hence, when
604 considering the P-dynamics observed seasonally the composition of the plankton community in
605 terms of both phytoplankton and bacteria needs to be considered.

606 **4.2. Seasonal changes in Phosphate uptake and DOP release in the Celtic Sea**

607 Observations from November to July in the Celtic Sea showed clear seasonal patterns in plankton
608 community composition (Mayers et al., this issue; Giering et al., this issue) and biogeochemical
609 processes (Garcia-Martin et al., this issue-A & B). Phytoplankton biomass (Chl-*a* and C_{phyto}) and

610 NPP both peaked in April and diverged in November and July, with Chl-*a* levels halved in July
611 relative to November, although levels of C_{phyto} and NPP were more similar (Tables 1 and 2). This
612 divergence is linked to seasonality in C to Chl-*a* ratios at CCS; using the cruise average values for
613 C_{phyto} and Chl-*a* from Table 2, we calculated C:Chl-*a* ratios (g:g) of 16 for November, 26 for April
614 and 53 for July. Such estimates are similar to those made by Holligan et al. (1984) for summer in
615 the Celtic Sea, and are driven by cellular responses to seasonal variability in resource (light,
616 nutrients) availability (Geider, 1987; Artega et al., 2016).

617 Seasonality in C:Chl-*a* ratios in the Celtic Sea link to variability in P_i (and NO_x) concentrations and
618 average surface mixed layer irradiances (\bar{E}_{SML} ; Table 1); with low \bar{E}_{SML} and high P_i in November
619 and high \bar{E}_{SML} and low P_i in July. Phytoplankton dynamics in autumn may be considered light-
620 driven while summer was nutrient-driven, with spring a transition between these two. Light levels
621 (\bar{E}_{SML}) in November were low (average: $1.9 \text{ mol quanta m}^{-2} \text{ d}^{-1}$, Table 1), only slightly above the
622 critical compensation irradiance for net growth in North Atlantic phytoplankton communities (1.3
623 $\text{mol quanta m}^{-2} \text{ d}^{-1}$, Siegel et al., 2002), and lower than levels suggested to limit Southern Ocean
624 communities ($3 \text{ mol quanta m}^{-2} \text{ d}^{-1}$, Venables and Moore, 2010). Nitrogen (nitrate, NO_x) availability
625 has been proposed previously to limit primary production during summer in the Celtic Sea
626 (Pemberton et al., 2004; Davis et al., 2014). Low N^* values seen at CCS support such a conclusion,
627 along with depletion of NO_x below detection levels ($<20 \text{ nM}$) in July whilst P_i remained above 55
628 nM (Table 1).

629 As well as phytoplankton biomass (Chl-*a*, C_{phyto}) and NPP, particulate organic phosphorus (POP)
630 also peaked in April (average: $2.3 \text{ mmol P m}^{-2}$) whilst concentrations in November and July were
631 relatively similar (1.4 and $1.5 \text{ mmol P m}^{-2}$, respectively) (Table 2). Cruise averages (and ranges) for
632 euphotic zone integrated DOP concentrations (Table 2) were twice as high in November (11 - 25
633 mmol P m^{-2}) relative to April (6 - 13 mmol P m^{-2}) and July (3 - 10 mmol P m^{-2}), with the summer
634 values the lowest overall. This is the same pattern as seen by Davis et al. (this issue) for the SML in
635 the Celtic Sea from a larger number of stations, with summer conditions also associated with the
636 lowest water-column (0-150 m) integrated DOP. Lower DOP concentrations in summer are likely to
637 be associated with the lower production rates (Fig. 4a, Table 2) and advective losses, as well as the
638 possible utilization of DOP (see Davis et al., this issue), which may occur in severely P-stressed
639 conditions (Dyhrman and Ruttenberg, 2006; Dyhrman et al., 2007; Duhamel et al., 2014). Summation
640 of the different P pools (P_i , POP and DOP) at CCS shows only a slight decline in the total P pool
641 over time (averages: 29.4 to $24.2 \text{ mmol P m}^{-2}$ from November to April, down to $12.2 \text{ mmol P m}^{-2}$ in
642 July). The proportion of total P in the DOP and P_i pools remained 45 to 56% and 34 to 39%,
643 respectively, while the fraction in the POP pool increased slightly from 5% in autumn to 14% in

644 summer (data not shown). Hence, there was a loss of P from the euphotic zone that may have been
645 linked to the sinking of particulate material below the thermocline and/or the advection of semi-
646 labile DOP (Reynolds et al., 2014; Davis et al., this issue).

647 April was also associated with a peak in P_i -uptake, with rates in July four times higher than those in
648 November, despite the reduced nutrient concentrations and P_i pool size (Tables 1 and 2). The
649 affinity of the plankton community for P_i -uptake can be assessed by examining the biomass-specific
650 turnover rate ($1/P_i$ turnover \times POP), where biomass is represented by POP and the units are
651 proportional to the volume of water cleared of substrate per unit biomass per unit time (Thingstad
652 and Rassoulzadegan, 1999; Tambi et al., 2009). For CCS, average values calculated this way for
653 November were $1.1 \text{ L pmol P}^{-1} \text{ h}^{-1}$ and were 5-times higher in April ($5.4 \text{ L pmol P}^{-1} \text{ h}^{-1}$) and 10-
654 times higher in July ($11.1 \text{ L pmol P}^{-1} \text{ h}^{-1}$); indicating that the affinity for P_i -uptake was highest in
655 summer rather than spring. The amount of this P_i taken up by the plankton that was then released as
656 DOP varied considerably between April and July, with the percentage extracellular release of DOP
657 highest in November (31-58%), then declining in April (7-45%) to a minimum in July (2-11%)
658 (Table 2).

659 To conclude, the summertime planktonic ecosystem in the Celtic Sea was highly efficient at P_i -
660 uptake and P-retention when P_i concentrations were low, and N-availability limited ecosystem
661 productivity. Such a system, with a high biomass-normalised affinity for P_i -uptake, had high rates
662 of recycling supporting relatively high rates of NPP (and P_i -uptake). Rates of NPP in summer were
663 also supported by regenerated sources of N rather than inorganic forms (Humphreys et al., this
664 issue). In contrast, the autumn ecosystem was the least efficient at P_i -uptake or P-retention, with
665 light as the most likely limiting factor for this community. In autumn, P_i -concentrations were also
666 relatively high and sufficient to support the low rates of NPP and P_i -uptake observed, with a
667 potentially light-limited system with a low affinity for P-cycling. Spring was a transitional period,
668 with the ecosystem evolving from a light-limited system as the water-column stratified and rates of
669 P_i -uptake and DOP production increased. The latter half of spring differs from the summer, as
670 despite the decline in P_i concentrations, P-retention remained low whilst summer conditions were
671 associated with efficient P-retention. The later stages of the spring bloom does not appear to be
672 characterised by well-developed P-recycling mechanisms, and DOP production may be driven by
673 high mortality related losses due to zooplankton (Mayers et al., this issue).

674 ***4.3. Seasonal changes in the turnover of the different P pools in the Celtic Sea***

675 Consideration of pool sizes and uptake rates only gives limited insights into biogeochemical
676 processes. Rather, consideration of the turnover rates of the different pools accounts for both the

677 relative pool size and uptake rate, providing further information on the dynamics of the system
678 (Benitez-Nelson, 2000). Short turnover times (a few hours or days) implies rapid biological
679 utilization, whilst longer turnover times (weeks or longer) indicate a lack of bioavailability or lower
680 requirements (Benitez-Nelson, 2000). Comparison of turnover times of related pools (e.g., C_{phyto}
681 and POC; Poulton et al., 2006) may also provide further insights into underlying ecological and
682 biogeochemical processes.

683 Phytoplankton turnover times, calculated from C_{phyto} and NPP (following Leynaert et al., 2000; see
684 also Poulton et al., 2006), show strong seasonality with short turnover times (<1 day) in April
685 compared with longer turnover times in both November and July (1.5-2.2 d and 1.1-4.4 d,
686 respectively) (Table 3). This seasonality in phytoplankton turnover times supports the suggestion of
687 light-limited growth in autumn and nutrient-stress in summer, as well as the rapid development of
688 the spring bloom through April (Table 2; see also Mayers et al., this issue; Garcia-Martin et al., this
689 issue-B). Inefficient utilization of the P_i pool in autumn relative to efficient utilization in spring and
690 summer is also supported by the seasonal differences in turnover times of this pool; from 21.9 to
691 42.3 d in November to 2.7 to 8.8 d in July, with turnover times in April declining from 8.9 d to 2.2
692 d (Table 3).

693 Turnover of the POP pool was slowest in November (2.8-4.9 d), with slightly faster turnover of
694 C_{phyto} (average 1.7 d) relative to POP (average 3.9 d), which may be indicative of plankton other
695 than phytoplankton (i.e., heterotrophic bacteria) strongly contributing to the POP pool. The
696 relatively rapid turnover of P_i and POP during summer and late spring, when P_i concentrations were
697 depleted (<10 mmol P m⁻²; Table 2), also implies efficient P-recycling (Benitez-Nelson and
698 Buesseler, 1999), even though these turnover times are longer than the very rapid turnover (<1 d)
699 observed in P-limited open-ocean regions (e.g., Sohm and Capone, 2010). This efficient P-recycling
700 in the Celtic Sea during summer, as well as utilisation of regenerated forms of N (Humphreys et al.,
701 this issue), supported similar levels of NPP to autumn, as well as relatively high rates of P_i -uptake
702 despite the seasonal differences in P_i availability (Table 2).

703 Turnover times for POP in April and July were surprisingly similar (0.5-1.3 d and 1.0-1.4 d,
704 respectively) when considering the much longer C_{phyto} turnover times in July (1.1-4.4 d; Table 3).
705 One interpretation of this discrepancy is that the two pools were composed of different components
706 during July, for example a greater heterotrophic bacterial contribution (or activity) in July than
707 November or April. Estimates of euphotic zone integrated bacterial biomass (C_{bact} ; Table 2) were
708 very similar in autumn and summer, and highest in spring. However, bacterial growth efficiency,
709 due to low respiratory C-losses and high C-fixation, were highest in July ($61 \pm 5\%$) rather than in
710 November ($27 \pm 3\%$) or April ($36 \pm 6\%$) (Garcia-Martin et al., this issue-A). Though summer C_{bact}

711 was similar to levels seen in autumn (and lower than in spring), its turnover time was much shorter
712 in summer; combining average values of bacterial production (see Garcia-Martin et al. this issue-A)
713 with average integrated bacterial biomass (Table 2) gives turnover times of 1.2 d in July, 4.7 d in
714 November and 5.6 d in April. These C_{bact} turnover times are similar to those for the POP pool in
715 both July and November (1.1 d and 3.9 d, respectively), but not in April (0.9 d) (Table 3). These
716 similarities likely indicate a significant bacterial contribution to both P_i -uptake rates and the POP
717 pool in summer and autumn. Though C_{bact} increased relative to C_{phyto} in spring (Table 2), bacterial
718 production remained low due to low growth efficiencies (Garcia-Martin et al., this issue-A),
719 suggesting that bacteria had less influence on P_i -uptake in spring than in autumn or summer.

720 The turnover times for the DOP pool were much longer (>40 d) than those for the other pools
721 (Table 3), although much shorter turnover (<10 d) did occur during late April. Slow turnover of
722 DOP in November was driven by relatively high DOP concentrations (11-25 mmol P m⁻²) and
723 moderate DOP production (0.11-0.28 mmol P m⁻² d⁻¹), although this sampling period also had the
724 highest overall relative percentage extracellular release (31-58%) (Table 3). July had similar slow
725 rates of DOP turnover to November (Table 3), although lower DOP concentrations and DOP
726 production rates (and the lowest overall extracellular release, ranging from 2-11%) (Table 2).
727 Hence, during both autumn and summer the DOP pool was largely inactive, with a large pool size
728 relative to low rates of DOP production. A contrasting situation was found in the Celtic Sea during
729 spring, especially during the latter half of the bloom where concentrations of P_i declined below 10
730 mmol P m⁻² (<200 nmol P L⁻¹) and DOP production rates increased above ~ 0.5 mmol P m⁻² d⁻¹
731 (Tables 1 and 2). Relatively short turnover times (range 4-17 d; Table 3) during the latter half of
732 April could potentially indicate a degree of DOP utilization by the plankton community during the
733 latter stages of the spring bloom, as inorganic nutrient sources declined (and both C_{phyto} and C_{bact}
734 increased; Table 2), and where the bioavailability of DOP may have increased (see Björkman et al.,
735 2000; Björkman and Karl, 2003).

736 The turnover times of the different C and P pools in the Celtic Sea provide support to the
737 suggestions of seasonal patterns in resource availability and their influence on P dynamics. Slow P_i
738 turnover in autumn was caused by the low-affinity ecosystem present, with inefficient P-dynamics
739 driven by light-limitation. In spring and summer, P_i availability became increasingly important with
740 a succession to a summer-time high-affinity ecosystem and efficient P dynamics. Summer was also
741 potentially associated with a strong bacterial influence on P dynamics. DOP turnover was relatively
742 slow throughout spring, summer and fall, indicating little biological utilization of this P-pool. The
743 lack of accumulation of DOP during summer contrasts with a previous Celtic Sea study by Davis et
744 al. (2014), potentially due to the low production rates observed in summer in this study.

745 **4.4. Seasonality in particulate stoichiometry in the Celtic Sea**

746 The last two sections have highlighted how seasonal variability in P_i -uptake and P-retention in the
747 Celtic Sea is related to both the composition of the plankton community (C_{phyto} , C_{bact}) and resource
748 (P_i , light) availability. Light-limitation led to an ecosystem composed of slow growing
749 phytoplankton and bacteria with inefficient P_i -uptake or P-retention. Low nutrient concentrations
750 (P_i , NO_x) in summer led to an efficient recycling ecosystem with slow-growing phytoplankton and
751 fast-growing bacteria influencing both high P_i -uptake and low DOP production. The spring bloom
752 was transitional between these two situations, with fast growing phytoplankton dominating P_i -
753 uptake and increasing DOP production as nutrient availability declined (P_i , NO_x). Such seasonal
754 variability in P_i -uptake, DOP production, plankton composition and NPP (C-fixation) will all result
755 in variability in the stoichiometric ratio of planktonic C to P uptake.

756 Taking the ratio of NPP to P_i -uptake (mol:mol) as indicative of the planktonic C:P (i.e. DIC: P_i)
757 uptake ratio shows clear seasonality (Table 3). Average ratios of NPP: P_i -uptake for each sampling
758 period ranged from 132 (range: 75-188) in November, to 116 (54-256) in April and 44 (21-53) in
759 July. Relative to the Redfield ratio (106:1), these ratios indicate a seasonal transition from slightly
760 C-rich uptake in autumn (and late spring) to strongly P-rich uptake in summer (and early spring)
761 (Table 3). If total P_i -uptake (i.e., $tP_i = P_i\text{-uptake} + \text{DOP production}$) is considered, then the
762 relatively high percentage extracellular release of DOP during autumn and late spring lead to C:P
763 ratios which are strongly P-rich relative to the Redfield ratio; with cruise averages of 81 (range: 37-
764 123) in November, 90 (46-195) in April and 42 (20-68) in July (Table 3). However, whether net or
765 total P_i -uptake are considered, autumn and spring are still, on average, more C-rich in their uptake
766 rates than summer, which was more P-rich.

767 In autumn, NPP: P_i -uptake ratios close to (and slightly higher) than the Redfield ratio were
768 associated with an ecosystem which was potentially light-limited, with low rates of NPP and P_i -
769 uptake, high DOP production and, though growing slowly, a bacterial influence. The spring bloom
770 was associated with a transition from light-limitation to low nutrient conditions as P_i concentrations
771 declined, with rapid phytoplankton turnover times (i.e., fast growth rates) slowing as resource
772 availability declined. NPP increased to a peak in spring and then declined slightly with nutrient
773 concentrations, whereas P_i -uptake remained high despite the decline in nutrient concentrations
774 (Tables 1 and 2). The ratio of NPP: P_i -uptake was low (P-rich) during early spring in association
775 with rapid phytoplankton growth rates, as is expected in nutrient-replete and optimal growth
776 conditions (Sterner and Elser, 2002), and then the ratio increased (C-rich) as growth slowed and
777 nutrient levels declined (Tables 2 and 3). This pattern in C:P uptake stoichiometry, from P-rich
778 organic matter formation in early spring to C-rich production in late spring, agrees well with

779 Humphreys et al. (this issue), who came to the same conclusion based on nutrient and dissolved
780 inorganic carbon dynamics during April.

781 The low NPP:P_i-uptake ratios (P-rich) in summer were not associated with rapid phytoplankton
782 growth (Table 3), but rather with high bacterial growth rates and a stronger bacterial influence on
783 C:P uptake (and retention). Heterotrophic bacteria are recognised as strong competitors for P_i under
784 nutrient depleted conditions (Thingstad et al., 1993, 1996; Duhamel and Moutin, 2009). Whilst
785 phytoplankton cellular C:P stoichiometry is near, or slightly lower, than the Redfield ratio (Geider
786 and LaRoche, 2002; Ho et al., 2003), bacterial cellular C:P ratios are significantly more P-rich (e.g.,
787 ~50; Fagerbakke et al., 1996; Sterner and Elser, 2002; Hessen et al., 2004; Duhamel and Moutin,
788 2009; see also Scott et al., 2012). Thus, it is suggested that the relatively P-rich uptake ratios in
789 summer relate to a stronger bacterial influence on P_i-uptake through increased competition as P_i
790 availability was low, bacterial growth efficiency was high (Garcia-Martin et al., this issue-A) and
791 phytoplankton growth rates were relatively low.

792 *4.5. Implications for the Continental Shelf Pump*

793 When considering the Continental Shelf Pump (CSP), C-overconsumption relative to nutrient
794 utilization (N, P) is an important factor in regulating the magnitude and efficiency of the CSP. Such
795 C-overconsumption has been suggested to occur during the nutrient-impooverished summer period,
796 when nutrient-starved phytoplankton may have high cellular C:P and excrete C-rich dissolved
797 organic matter (Toggweiler et al., 1993; Thomas et al., 2004, 2005; Bozec et al., 2006; Kühn et al.,
798 2010). In the Celtic Sea, Davis et al. (this issue) observed that both the particulate and dissolved
799 pools showed seasonal succession in becoming increasingly C-rich relative to the Redfield ratio
800 from autumn through spring and into summer. In this context, our observations of P-rich uptake in
801 July may appear paradoxical, however what they imply is that significantly more C-rich
802 biogeochemical processes must be balancing out the influence of plankton uptake stoichiometry on
803 particulate and dissolved organic matter stoichiometry.

804 In the case of particulate material in summer, when bacteria appear to dominate P-uptake and
805 retention, other components of the plankton (phytoplankton, zooplankton), as well as detrital
806 material, may all be relatively C-rich. Slow-growing phytoplankton in summer (Table 3) still
807 represented more biomass than bacteria ($C_{\text{bact}}:C_{\text{phyto}} \sim 0.17-0.37$) and hence may be more influential
808 on particulate stoichiometry than nutrient recycling. For the dissolved pool in summer, the plankton
809 community may excrete large quantities of dissolved organic carbon (see Garcia-Martin et al., this
810 issue A), whereas our observations indicate that they are releasing very little in terms of DOP.
811 Hence, the dissolved organic matter pool in summer will become strongly enriched in C, with

812 results from Davis et al. (this issue) showing the summertime DOM pool had C:P ratios 3 times
813 higher than the Redfield ratio (see also Humphreys et al., this issue). Overall, our results have two
814 important implications for the CSP: 1) both autotrophs and heterotrophs seasonally influence
815 nutrient (P, N) recycling and uptake (C:P) stoichiometry, and 2) there is a tendency for uptake (C:P)
816 stoichiometry to be nutrient-rich rather than strongly C-rich, as would be expected to support an
817 efficient CSP. Hence, for a nutrient-efficient CSP (and C-overconsumption), other biogeochemical
818 processes involved (e.g. DOM production, particulate remineralisation) need to be relatively C-rich
819 to balance out the influence of uptake stoichiometry.

820 **5. Conclusions**

821 In this study, seasonal variability in P_i -uptake and DOP production in the Celtic Sea was related to
822 both the composition of the plankton community (C_{phyto} , C_{bact}) and resource (P_i , light, NO_x)
823 availability. In autumn, light-limitation led to an ecosystem composed of slow-growing
824 phytoplankton and bacteria with relatively low P_i -uptake and with high DOP production. In
825 summer, low nutrients (low P_i , depleted NO_x) led to an efficient recycling ecosystem supporting
826 relatively high NPP with slow-growing phytoplankton, and fast-growing bacteria influencing high
827 P_i -uptake and low DOP production. The spring bloom in the Celtic Sea was transitional between
828 these two situations, with fast-growing phytoplankton dominating P_i -uptake with increasing DOP
829 production (in absolute and relative terms) as inorganic nutrients declined (P_i , NO_x) towards the
830 latter stages of the bloom.

831 These seasonal changes in ecosystem dynamics were associated with changes in the ratio of C to P
832 uptake, as described by the ratio of NPP to P_i -uptake in this study, with the summer relatively more
833 P-rich in terms of uptake than autumn or spring. Such P-rich uptake was associated with a stronger
834 influence of actively growing heterotrophic bacteria rather than phytoplankton activity, whereas P-
835 rich uptake in early spring was associated with fast phytoplankton growth in optimal growth
836 (bloom) conditions. In terms of our original hypotheses, P-rich uptake associated with fast
837 phytoplankton growth in the spring bloom goes against the first hypothesis (i.e. that optimal growth
838 conditions in spring would lead to uptake stoichiometry in Redfield proportions), and rather
839 supports the 'growth-rate hypothesis' of Sterner and Elser (2002). Whilst departures from the
840 Redfield ratio in uptake stoichiometry did occur in response to changes in resource (light, nutrients)
841 availability (the second hypothesis), such departures were also associated with different seasonal
842 influences of autotrophs and heterotrophs. Hence, our results highlight the importance of
843 considering the full plankton community in terms of seasonal P-dynamics, and in the underlying
844 mechanisms supporting the CSP.

845 **Acknowledgements**

846 The authors would like to acknowledge the support of the captains, officers and crews of the
847 associated Shelf Sea Biogeochemistry cruises, as well as J. Sharples and M. Moore who acted as the
848 Principal Scientific Officers for the November and July cruises. This study was supported by the
849 UK Natural Environmental Research Council via the Shelf Sea Biogeochemistry research
850 programme, through grants NE/K001701/1, NE/K002007/1 and NE/K002058/1. KM was supported
851 by a NERC Doctoral Training Partnership (DTP) studentship as part of the Southampton
852 Partnership for Innovative Training of Future Investigators Researching the Environment
853 (SPITFIRE).

854 **References**

- 855 Arrigo, K.R., 2005. Marine microorganisms and global nutrient cycles. *Nature* 437, doi:
856 10.1038/nature04159.
- 857 Arteaga, L., Pahlow, M., Oschlies, A., 2016. Modeled Chl:C ratio and derived estimates of
858 phytoplankton carbon biomass and its contribution to total particulate organic carbon in the
859 global surface ocean. *Global Biogeochemical Cycles*, 30, doi: 10.1002/2016GB005458.
- 860 Bauer, J.E., Cai, W.-J., Raymond, P.A., Bianchi, T.S., Hopkinson, C.S., Regnier, P.A.G., 2013. The
861 changing carbon cycle of the coastal ocean. *Nature Geoscience* 504, 61-70.
- 862 Benitez-Nelson, C.R., 2000. The biogeochemical cycling of phosphorus in marine systems. *Earth-*
863 *Science Reviews* 51, 109-135.
- 864 Benitez-Nelson, C.R., Buesseler, K.O., 1999. Variability in inorganic and organic phosphorus
865 turnover rates in the coastal ocean. *Nature* 398, 502-505.
- 866 Björkman, K.M., Thomson-Bulldis, A.L., Karl, D.M., 2000. Phosphorus dynamics in the North
867 Pacific subtropical gyre. *Marine Ecology Progress Series* 22, 185-198.
- 868 Björkman, K.M., Karl, D.M., 2003. Bioavailability of dissolved organic phosphorus in the euphotic
869 zone at Station ALOHA, North Pacific Subtropical Gyre. *Limnology and Oceanography* 48,
870 1049-1057.
- 871 Bozec, Y., Thomas, H., Schiettecatte, L.-S., Borges, A.V., Elkalay, K., de Baar, H.J.W., 2006.
872 Assessment of the processes controlling seasonal variations of dissolved inorganic carbon in the
873 North Sea. *Limnology and Oceanography* 51, 2746-2762.
- 874 Burkhardt, B.G., Watkins-Brandt, K.S., Defforey, D., Paytan, A., White, A.E., 2014.
875 Remineralization of phytoplankton-derived organic matter by natural populations of
876 heterotrophic bacteria. *Marine Chemistry* 163, 1-9.

- 877 Davis, C.E., Mahaffey, C., Wolff, G.A., Sharples, J., 2014. A storm in a shelf sea: Variability in
878 phosphorus distribution and organic matter stoichiometry. *Geophysical Research Letters* 41, doi:
879 10.1002/2014GL061949.
- 880 Davis, C.E., Blackbird, S., Wolff, G.A., Sharples, J., Woodward, E.M.S., Mahaffey, C. Seasonal
881 organic matter dynamics in a temperate shelf sea. *Progress in Oceanography*, this issue.
- 882 Donald, K.M., Joint, I., Rees, A.P., Woodward, E.M.S., Savidge, G., 2001. Uptake of carbon,
883 nitrogen and phosphorus by phytoplankton along the 20°W meridian in the NE Atlantic between
884 57.5°N and 37°N. *Deep-Sea Research II* 48, 873-897.
- 885 Duhamel, S., Moutin, T., 2009. Carbon and phosphate incorporation rates of microbial assemblages
886 in contrasting environments in the Southeast Pacific. *Marine Ecology Progress Series* 375, 53-
887 64.
- 888 Duhamel, S., Björkman, K.M., Karl, D.M., 2012. Light dependence of phosphorus uptake by
889 microorganisms in the subtropical North and South Pacific Ocean. *Aquatic Microbial Ecology*
890 67, 225-238.
- 891 Duhamel, S., Björkman, K.M., Doggett, J.K., Karl, D.M., 2014. Microbial response to enhanced
892 phosphorus cycling in the North Pacific Subtropical Gyre. *Marine Ecology Progress Series* 504,
893 43-58.
- 894 Dyrman, S.T., Ammerman, J.W., Van Mooy, B.A.S., 2007. Microbes and the marine phosphorus
895 cycle. *Oceanography* 20, 110-116.
- 896 Dyrman, S.T., Ruttenberg, K.C., 2006. Presence and regulation of alkaline phosphatase activity in
897 eukaryotic phytoplankton from the coastal ocean: Implications for dissolved organic phosphorus
898 remineralization. *Limnology and Oceanography* 51, 1381-1390.
- 899 Elser, J.J., Kyle, M., Makino, W., Yoshida, T., Urabe, J., 2003. Ecological stoichiometry in the
900 microbial food web: a test of the light: nutrient hypothesis. *Aquatic Microbial Ecology* 31, 49-
901 65.
- 902 Faggebakke, K.M., Heldal, M., Norland, S., 1996. Content of carbon, nitrogen, oxygen, sulfur and
903 phosphorus in native aquatic and cultured bacteria. *Aquatic Microbial Ecology* 10, 15-27.
- 904 Falkowski, P.G., 2000. Rationalizing elemental ratios in unicellular algae. *Journal of Phycology* 36,
905 3-6.
- 906 Falkowski, P.G., Davis, C.S., 2004. Natural proportions. *Nature* 431, 131.
- 907 Finkel, Z.V., Beardall, J., Flynn, K.J., Quigg, A., Rees, T.A.V., Raven, J.A., 2010. Phytoplankton in
908 a changing world: cell size and elemental stoichiometry. *Journal of Plankton Research* 32, 119-
909 137.
- 910 García-Martín, E.E., Daniels, C.J., Davidson, K., Davis, C.E., Mahaffey, C., Mayers, K.M.J.,
911 McNeil, S., Poulton, A.J., Purdie, D.A., Tarran, G., Robinson, C. Seasonal changes in

- 912 microplankton respiration and bacterial metabolism in a temperate Shelf Sea. Progress in
913 Oceanography, this issue-A.
- 914 García-Martín, E.E., Daniels, C.J., Davidson, K., Lozano, J., Mayers, K.M.J., McNeil, S., Mitchell,
915 E., Poulton, A.J., Purdie, D.A., Tarran, G., Whyte, C., Robinson, C. Plankton community
916 respiration and bacterial metabolism in a North Atlantic shelf sea during spring bloom
917 development (April 2015). Progress in Oceanography, this issue-B.
- 918 Geider, R., 1987. Light and temperature dependence of the carbon to chlorophyll-a ratio in
919 microalgae and cyanobacteria: implications for physiology and growth of phytoplankton. *New*
920 *Phytologist* 106, 1-34.
- 921 Geider, R., La Roche, J., 2002. Redfield revisited: variability of C:N:P in marine microalgae and its
922 biochemical basis. *European Journal of Phycology* 37, 1-17.
- 923 Giering, S.L.C., Wells, S.R., Mayers, K.M.J., Schuster, H., Cornwell, L., Fileman, E., Atkinson, A.,
924 Cook, K.B., Preece, C., Mayor, D.J. Seasonal variation of zooplankton community structure and
925 trophic position in the Celtic Sea: a stable isotope and biovolume spectrum approach. Progress in
926 Oceanography, this issue.
- 927 Hessen, D.O., Færøvig, P.J., Andersen, T., 2002. Light, nutrients, and P:C ratios in algae: Grazer
928 performance related to food quality and quantity. *Ecology* 83, 1886-1898.
- 929 Hessen, D.O., Ågren, G.I., Anderson, T.R., Elser, J.T., de Ruiter, P.C., 2004. Carbon sequestration
930 in ecosystems: The role of stoichiometry. *Ecology* 85, 1179-1192.
- 931 Hickman, A.E., Moore, C.M., Sharples, J., Lucas, M.I., Tilstone, G.H., Krivtsov, V., Holligan,
932 P.M., 2012. Primary production and nitrate uptake within the seasonal thermocline of a stratified
933 shelf sea. *Marine Ecology Progress Series* 463, 39-57.
- 934 Ho, T-Y., Quigg, A., Finkel, Z.V., Milligan, A.J., Wyman, K., Falkowski, P.G., Morel, F.M.M.,
935 2003. The elemental composition of some marine phytoplankton. *Journal of Phycology* 39,
936 1145-1159.
- 937 Holligan, P.M., Harris, R.P., Newe, R.C., Harbour, D.S., Head, R.N., 1984. Vertical distribution
938 and partitioning of organic carbon in mixed, frontal and stratified waters of the English Channel.
939 *Marine Ecology Progress Series* 14, 111-127.
- 940 Humphreys, M.P., Achterberg, E.P., Chowdhury, M.Z.H., Griffiths, A.M., Hartman, S.E., Hopkins,
941 J.E., Hull, T., Kivimae, C., Smilenova, A., Wihsgott, J., Woodward, E.M.S., Moore, C.M.
942 Mechanisms for a nutrient-conserving carbon pump in a seasonally stratified, temperate
943 continental shelf sea. Progress in Oceanography, this issue.
- 944 Hydes, D.J., Aoyama, M., Aminot, A., Bakker, K., Becker, S., Coverly, S., Daniel, A., Dickson,
945 A.G., Grosso, O., Kerouel, R., van Ooijen, J., Sato, K., Tanhua, T., Woodward, E.M.S., Zhang,
946 J.Z., 2010. Determination of dissolved nutrients (N, P, Si) in seawater with high precision and

- 947 inter-comparability using gas-segmented continuous flow analysers. In: The GO-SHIP repeat
948 hydrography manual: A collection of expert reports and guidelines. IOCCP report No. 14, ICPO
949 publication series No. 134.
- 950 Joint, I., Wollast, R., Chou, L., Batten, S., Elskens, M., Edwards, E., Hirst, A., Burkill, P., Groom ,
951 S., Gibb, S., Miller, A., Hydes, D., Dehairs, F., Antia, A., Barlow, R., Rees, A., Pomroy, A.,
952 Brockmann, U., Cummings, D., Lampitt, R., Loijens, M., Mantoura, F., Miller, P., Raabe, T.,
953 Alvarez-Salgado, X., Stelfox, C., Woolfenden, J., 2001. Pelagic production at the Celtic Sea
954 shelf break. *Deep-Sea Research Part II* 48, 14-15.
- 955 Karl, D.M., 2000. Phosphorus, the staff of life. *Nature* 406, 31-33.
- 956 Karl, D.M., Tien, G., 1992. MAGIC: A sensitive and precise method for measuring dissolved
957 phosphorus in aquatic environments. *Limnology and Oceanography* 37, 103-116.
- 958 Karl, D.M., Björkman, K.M., Dore, J.E., Fujieki, L., Hebel, D.V., Houlihan, T., Letelier, R.M.,
959 Tupas, L.M., 2001. Ecological nitrogen-to-phosphorus stoichiometry at station ALOHA. *Deep
960 Sea Research II* 48, 1529-1566.
- 961 Kovala, P.E., Larrence, J.D., 1966. Computation of phytoplankton number, cell volume, cell surface
962 and plasma volume per litre, from microscopic counts. Special Report No. 38, Department of
963 Oceanography, University of Washington.
- 964 Krom, M.D., Kress, N., Brenner, S., Gordon, L.I., 1991. Phosphorus limitation of primary
965 productivity in the eastern Mediterranean Sea. *Limnology and Oceanography* 36, 424-432.
- 966 Kühn, W., Pätsch, J., Thomas, H., Borges, A.V., Schiettecatte, L-S., Bozec, Y., Prowe, A.E.F.,
967 2010. Nitrogen and carbon cycling in the North Sea and exchange with the North Atlantic – A
968 model study, Part II: Carbon budget and fluxes. *Continental Shelf Research* 30, 1701-1716.
- 969 Leynaert, A., Tréguer, P., Lancelot, C., Rodier, M., 2001. Silicon limitation of biogenic silica
970 production in the Equatorial Pacific. *Deep-Sea Research I* 48, 639-660.
- 971 Lønborg, C., Davidson, K., Álvarez-Salgado, X.A., Miller, A.E.J., 2009. Bioavailability of bacterial
972 degradation rates of dissolved organic matter in a temperate coastal area during an annual cycle.
973 *Marine Chemistry* 113, 219-226.
- 974 Lomas, M.W., Burke, A.L., Lomas, D.A., Bell, D.W., Shen, C., Dyrman, S.T., Ammerman, J.W.,
975 2010. Sargasso Sea phosphorus biogeochemistry: an important role for dissolved organic
976 phosphorus (DOP). *Biogeosciences* 7, 695-710.
- 977 Lopez, J., Garcia, N.S., Talmy, D., Martiny, A.C., 2016. Diel variability in the elemental
978 composition of the marine cyanobacterium *Synechococcus*. *Journal of Plankton Research* 38,
979 1052-1061.
- 980 López-Sandoval, D.C., Fernández, A., Marañón, E., 2011 Dissolved and particulate primary
981 production along a longitudinal gradient in the Mediterranean Sea. *Biogeosciences* 8, 815-825.

- 982 Mayers, K.M.J., Poulton, A.J., Daniels, C.J, Wells, S.R., Woodward, E.M.S., Tyrrell, T., Giering,
983 S.L.C. Top-down control of coccolithophore populations during spring in a temperate Shelf Sea
984 (Celtic Sea, April 2015). *Progress in Oceanography*, this issue.
- 985 Moore, C.M., Mills, M.M., Achterberg, E.P., Geider, R.J., LaRoche, J., Lucas, M.I., McDonagh,
986 E.L., Pan, X., Poulton, A.J., Rijkenberg, M.J.A., Suggett, D.J., Ussher, S.J., Woodward, E.M.S.,
987 2009. Large-scale distribution of Atlantic nitrogen fixation controlled by iron availability. *Nature*
988 *Geoscience* 2, 867-871.
- 989 Moore, C.M., Mills, M.M., Arrigo, K.R., Berman-Frank, I., Bopp, L., Boyd, P.W., Galbraith, E.D.,
990 Geider, R.J., Guieu, C., Jaccard, S.L., Jickells, T.D., La Roche, J., Lenton, T.M., Mahowald,
991 N.M., Maranon, E., Marinov, I., Moore, J.K., Nakatsuka, Oschlies, A., Saito, M.A., Thingstad,
992 T.F., Tsuda, A., Ulloa, O., 2013. *Nature Geoscience* 6, 701-710, doi: 10.1038/ngeo1765.
- 993 Murphy, J., Riley, J.P., 1962. A modified single solution method for the determination of phosphate
994 in natural waters. *Analytica Chimica Acta* 27, 31-36.
- 995 Pemberton, K., Rees, A.P., Miller, P.I., Raine, R., Joint, I., 2004. The influence of water body
996 characteristics on phytoplankton diversity and production in the Celtic Sea. *Continental Shelf*
997 *Research* 24, 2011-2028.
- 998 Popendorf, K.J., Duhamel, S., 2015. Variable phosphorus uptake rates and allocation across
999 microbial groups in the oligotrophic Gulf of Mexico. *Environmental Microbiology* 17, 3992-
1000 4006.
- 1001 Poulton, A.J., Sanders, R., Holligan, P.M., Stinchcombe, M.C., Adey, T.R., Brown, L.,
1002 Chamberlain, K., 2006. Phytoplankton mineralization in the tropical and subtropical Atlantic
1003 Ocean. *Global Biogeochemical Cycles* 20, GB4002, doi: 10.1029/2006GB002712.
- 1004 Poulton, A.J., Stinchcombe, M.C., Achterberg, E.P., Bakker, D.C.E., Dumousseaud, C., Lawson
1005 H.E., Lee, G.A., Richier, S., Suggett, D.J., Young, J.R., 2014. Coccolithophores on the north-
1006 west European shelf: calcification rates and environmental controls. *Biogeosciences* 11, 3919-
1007 3940.
- 1008 Rees, A.P., Joint, I., Donald, K.M., 1999. Early spring bloom phytoplankton-nutrient dynamics at
1009 the Celtic Sea Shelf Edge. *Deep-Sea Research I* 46, 483-510.
- 1010 Redfield, A.C., Ketchum, B.H., Richards, F.A., 1963. The influence of organisms on the
1011 composition of seawater. In: *The sea* (ed. Hill, M.N.), Wiley, 26-77.
- 1012 Reynolds, S., Mahaffey, C., Roussenov, V., Williams, R.G., 2014. Evidence for production and
1013 lateral transport of dissolved organic phosphorus in the eastern subtropical North Atlantic.
1014 *Global Biogeochemical Cycles* 28, doi: 10.1002/2013GB004801.
- 1015 Richier, S., Achterberg, E.P., Dumousseaud, C., Poulton, A.J., Suggett, D.J., Tyrrell, T., Zubkov,
1016 M.V., Moore, C.M., 2014. Phytoplankton responses and associated carbon cycling during

- 1017 shipboard carbonate chemistry manipulation experiments conducted around Northwest European
1018 shelf seas. *Biogeosciences* 11, 4733-4752.
- 1019 Scott, J.T., Cotner, J.B., LaPara, T.M., 2012. Variable stoichiometry and homeostatic regulation of
1020 bacterial biomass elemental composition. *Frontiers in Microbiology* 3, 1-8.
- 1021 Siegal, D.A., Doney, S.C., Yoder, J.A., 2002. The North Atlantic spring phytoplankton bloom and
1022 Sverdrup's critical depth hypothesis. *Science*, 296, 730-733, doi: 10.1126/science.1069174.
- 1023 Simpson J.H., Sharples, J., 2012. Introduction to the physical and biological oceanography of shelf
1024 seas. Cambridge, Cambridge University Press. 424 pp.
- 1025 Sohm, J.A., Capone, D.G., 2010. Zonal differences in phosphorus pools, turnover and deficiency
1026 across the tropical North Atlantic Ocean. *Global Biogeochemical Cycles* 24, GB2008, doi:
1027 10.1029/2008GB003414.
- 1028 Stener, R.W., Elser, J.J., 2002. Ecological stoichiometry: The biology of elements from molecules
1029 to the biosphere. Princeton University, 464 pp.
- 1030 Talmy, D., Blackford, J., Hardman-Mountford, N.J., Polimene, L., Follows, M.J., Geider, R.J.,
1031 2014. Flexible C:N ratio enhances metabolism of large phytoplankton when resource supply is
1032 intermittent. *Biogeosciences* 11, 4881-4895.
- 1033 Tambi, H., Flaten, G.A.F., Egge, J.K., Bodtker, G., Jacobsen, T.F. Thingstad, 2009. Relationship
1034 between phosphate affinities and cell size and shape in various bacteria and phytoplankton.
1035 *Aquatic Microbial Ecology Special Issue* 3, 1-10.
- 1036 Tarran, G.A., Heywood, J.L., Zubkov, M.V., 2006. Latitudinal changes in the standing stocks of
1037 nano- and pico-eukaryotic phytoplankton in the Atlantic Ocean. *Deep-Sea Research II* 53, 1516-
1038 1529.
- 1039 Thingstad, T.F., Skjoldal E.F., Bohne, R.A., 1993. Phosphorus cycling and algal-bacterial
1040 competition in Sandsfjord, western Norway. *Marine Ecology Progress Series* 99, 239-259.
- 1041 Thingstad, T.F., Riemann, B., Havskum, H., Garde, K., 1996. Incorporation rates and biomass
1042 content of C and P in phytoplankton and bacteria in the Bay of Aarhus (Denmark) June 1992.
1043 *Journal of Plankton Research* 18, 97-121.
- 1044 Thingstad, T.F., Rassoulzadegan, F., 1999. Conceptual models for the biogeochemical role of the
1045 photic zone microbial food web, with particular reference to the Mediterranean Sea. *Progress in*
1046 *Oceanography* 44, 271-286.
- 1047 Thomson-Bulldis, A., Karl, D.M., 1998. Application of a novel method for phosphorus
1048 determinations in the oligotrophic North Pacific Ocean. *Limnology and Oceanography* 43, 1565-
1049 1577.
- 1050 Toggweiler, J.R., 1993. Carbon overconsumption. *Nature* 363, 210-211.

- 1051 Tomas, H., Bozec, Y., Elkalay, K., de Baer, H.J.W., 2004. Enhanced open ocean storage of CO₂
1052 from shelf sea pumping, *Science* 304, 1005-1008.
- 1053 Tomas, H., Bozec, Y., de Baar, H.J.W., Elkalay, K., Frankignoulle, M., Schiettecatte, L.-S.,
1054 Kattner, G., Borges, A.V., 2005. The carbon budget of the North Sea. *Biogeosciences* 2, 87-96.
- 1055 Venables, H.J., Moore, C.M., 2010. Phytoplankton and light limitation in the Southern Ocean:
1056 Learning from high-nutrient, high-chlorophyll areas. *Journal of Geophysical Research*, 115,
1057 C02015, doi: 10.1029/2009JC005361.
- 1058 Woodward, E.M.S., Rees, A.P., 2001. Nutrient distributions in an anticyclonic eddy in the North
1059 East Atlantic Ocean, with reference to nanomolar ammonium concentrations. *Deep-Sea*
1060 *Research II*, 48, 775-794.
- 1061 Widdicombe, C.E., Eloire, D., Harbour, D., Harris, R.P., Somerfield, P.J., 2010. Long-term
1062 phytoplankton community dynamics in the Western English Channel. *Journal of Plankton*
1063 *Research* 32, 643-655.
- 1064

1065 TABLES

1066 **Table 1.** Environmental characteristics at two study sites in the Celtic Sea for November (2014),
1067 April (2015) and July (2015). CCS, Central Celtic Sea study site; CS2, Shelf Edge study site;
1068 SML, surface mixed layer depth; SML Temp., average temperature of the SML; Zeup, depth of
1069 the euphotic zone; P_i , inorganic phosphate concentration; NO_x , concentration of nitrate+nitrite;
1070 N^* , ratio of nitrate+nitrite to phosphate expressed after Moore et al. (2009); E_0 , incidental
1071 irradiance (PAR) at the sea-surface; \bar{E}_{SML} , average irradiance (PAR) over the SML.

1072 **Table 2.** Euphotic zone inventories of biomass, production and phosphorus dynamics at two study
1073 sites in the Celtic Sea for November (2014), April (2015) and July (2015). CCS, Central Celtic
1074 Sea study site; CS2, Shelf Edge study site; Chl-*a*, chlorophyll-*a* concentrations; C_{phyto} ,
1075 phytoplankton biomass; C_{bact} , bacterial biomass; NPP, Net Primary Production; P_i , inorganic
1076 phosphate concentration; POP, particulate organic phosphate; DOP, dissolved organic
1077 phosphorus; P_i uptake, uptake of inorganic phosphate; DOP prod., production of DOP; PER,
1078 percentage extracellular release of DOP.

1079 **Table 3.** Turnover times and elemental stoichiometry at two study sites in the Celtic Sea for
1080 November (2014), April (2015) and July (2015). Stoichiometry of carbon fixation (net primary
1081 production, NPP) is expressed against P_i uptake and total P_i uptake (i.e. sum of P_i uptake + DOP
1082 production) on daily timescales. CCS, Central Celtic Sea study site; CS2, Shelf Edge study site;
1083 C_{phyto} , phytoplankton carbon; P_i , inorganic phosphate; POP, particulate organic phosphate; DOP,
1084 dissolved organic phosphorus; tP_i , total P_i uptake (sum of P_i -uptake and DOP production).

1085

1086 SUPPLEMENTARY TABLES

1087 **Table S1.** Irradiance in incubations.

Table 1. Environmental characteristics at two study sites in the Celtic Sea for November (2014), April (2015) and July (2015). CCS, Central Celtic Sea study site; CS2, Shelf Edge study site; SML, surface mixed layer depth; SML Temp., average temperature of the SML; Zeup, depth of the euphotic zone; P_i , inorganic phosphate concentration; NO_x , concentration of nitrate+nitrite; N^* , ratio of nitrate+nitrite to phosphate expressed after Moore et al. (2009); E_0 , incidental irradiance (PAR) at the sea-surface; \bar{E}_{SML} , average irradiance (PAR) over the SML.

Season / Date	Site	SML (m)	SML Temp. (°C)	Zeup (m)	P_i (nmol P L ⁻¹)	NO_x (μmol N L ⁻¹)	N^*	E_0 (mol PAR m ⁻² d ⁻¹)	\bar{E}_{SML}
<i>November 2014</i>									
10 Nov	CCS	44	13.7	40	180	2.1	-0.8	8.4	1.6
12 Nov	CCS	32	13.6	28	180	2.1	-0.8	11.9	2.3
18 Nov	CS2	58	13.9	65	280	3.5	-1.0	7.7	1.8
20 Nov	CS2	58	14.1	55	220	2.6	-1.0	9.3	1.9
22 Nov	CCS	54	13.1	43	210	1.8	-1.6	8.1	1.4
25 Nov	CCS	52	12.8	50	210	2.5	-0.9	12.1	2.5
Mean		50	13.5	47	213	2.4	-1.0	9.6	1.9
<i>April 2015</i>									
04 April	CCS	51	10.0	37	491	6.1	-1.8	20.7	3.3
06 April	CCS	47	10.0	37	459	5.7	-1.7	43.2	7.4
10 April	CS2	27	11.3	48	510	8.2	0.1	18.1	6.5
11 April	CCS	22	10.3	32	330	3.8	-1.5	42.3	12.8
15 April	CCS	25	10.6	28	190	1.2	-1.9	20.0	4.8
20 April	CCS	24	10.6	28	190	2.0	-1.0	41.4	10.3
24 April	CS2	24	11.7	30	190	2.3	-0.7	45.4	12.0
25 April	CCS	16	11.1	35	130	0.4	-1.7	42.0	17.5
Mean		30	10.7	34	311	3.7	-1.7	34.1	9.3
<i>July 2015</i>									
14 July	CCS	28	16.0	53	90	<0.02	-1.4	23.2	8.7
15 July	CCS	30	16.1	52	90	<0.02	-1.4	33.2	11.6
19 July	CS2	11	15.8	20	70	<0.02	-1.1	26.1	9.5
20 July	CS2	12	16.2	25	80	0.17	-1.1	49.8	20.1
24 July	CCS	22	16.8	55	80	<0.02	-1.3	26.2	12.0
29 July	CCS	35	16.2	46	60	<0.02	-0.9	41.5	11.5
30 July	CCS	43	16.3	46	55	<0.02	-0.9	49.4	11.3
Mean		26	16.2	42	76	0.04	-1.2	35.6	12.1

Table 2. Euphotic zone inventories of biomass, production and phosphorus dynamics at two study sites in the Celtic Sea for November (2014), April (2015) and July (2015). CCS, Central Celtic Sea study site; CS2, Shelf Edge study site; Chl-*a*, chlorophyll-*a* concentrations; C_{phyto} , phytoplankton biomass; C_{bact} , bacterial biomass; NPP, Net Primary Production; P_i , inorganic phosphate concentration; POP, particulate organic phosphate; DOP, dissolved organic phosphorus; P_i uptake, uptake of inorganic phosphate; DOP prod., production of DOP; PER, percentage extracellular release of DOP.

Season / Date	Site	Chl- <i>a</i> (mg m ⁻²)	C_{phyto} (mmol C m ⁻²)	C_{bact}	NPP (mmol C m ⁻² d ⁻¹)	P_i (mmol P m ⁻²)	POP	DOP	P_i uptake (mmol P m ⁻² d ⁻¹)	DOP prod. (mmol P m ⁻² d ⁻¹)	PER (%)	Chl- <i>a</i> normalised NPP (gC (g Chl- <i>a</i>) ⁻¹ h ⁻¹)
<i>November 2014</i>												
10 Nov	CCS	59.7	91	28	37.0	7.6	1.7	14	0.24	-	-	0.8
12 Nov	CCS	37.4	36	-	18.5	5.2	-	-	0.14	0.19	58	0.7
18 Nov	CS2	54.4	78	24	22.5	18.3	2.0	25	0.30	0.28	48	0.6
20 Nov	CS2	57.6	73	24	26.3	12.0	1.4	13	0.24	0.11	31	0.6
22 Nov	CCS	68.7	91	32	42.9	9.0	1.0	11	0.25	0.13	34	0.8
25 Nov	CCS	70.8	93	32	46.9	10.5	1.1	19	0.25	0.17	34	0.9
Mean		58.1	77	28	32.4	10.4	1.4	16	0.24	0.17	41	0.7
<i>April 2015</i>												
04 April	CCS	49.6	153	49	117.6	18.3	1.0	12	1.43	0.11	7	2.0
06 April	CCS	61.4	162	57	59.1	17.3	-	-	1.03	0.12	10	0.8
10 April	CS2	37.8	106	27	87.8	25.1	1.1	13	1.64	0.26	14	2.0
11 April	CCS	94.9	221	142	154.0	11.1	3.1	13	1.68	0.36	18	1.4
15 April	CCS	152.6	180	162	532.1	6.7	3.1	10	2.08	0.65	24	3.0
20 April	CCS	92.3	168	182	206.2	5.3	2.4	9	1.89	0.82	30	1.9
24 April	CS2	57.4	202	44	132.8	5.7	2.1	6	1.33	1.11	45	2.0
25 April	CCS	110.4	247	142	321.0	5.7	3.5	12	1.76	0.48	21	2.5
Mean		82.1	180	101	201.3	11.9	2.3	11	1.61	0.49	21	2.0
<i>July 2015</i>												
14 July	CCS	19.3	200	30	58.5	6.3	2.2	7	1.11	0.02	2	2.3
15 July	CCS	28.5	121	23	43.7	6.6	-	-	1.18	-	-	1.2
19 July	CS2	18.4	66	32	32.5	1.8	1.0	3	0.72	0.04	5	1.3
20 July	CS2	17.2	-	-	18.3	2.1	-	-	0.53	0.03	5	0.8
24 July	CCS	35.7	86	33	38.3	12.2	-	-	0.96	0.07	7	0.8
29 July	CCS	26.4	79	27	19.7	4.2	1.3	10	0.92	0.08	8	0.6
30 July	CCS	28.0	-	-	36.8	5.3	-	-	0.48	0.06	11	1.0
Mean		24.8	110	29	35.4	5.5	1.5	7	0.84	0.05	6	1.1

Table 3. Turnover times and uptake stoichiometry at two study sites in the Celtic Sea for November (2014), April (2015) and July (2015). Stoichiometry of carbon fixation (net primary production, NPP) is expressed against P_i uptake and total P_i uptake (i.e. sum of P_i uptake + DOP production) on daily timescales. CCS, Central Celtic Sea study site; CS2, Shelf Edge study site; C_{phyto} , phytoplankton carbon; P_i , inorganic phosphate; POP, particulate organic phosphate; DOP, dissolved organic phosphorus; tP_i , total P_i uptake (sum of P_i -uptake and DOP production).

Season / Date	Site	C_{phyto}	P_i	POP	DOP	Daily NPP: P_i uptake	Daily NPP: tP_i uptake
			[d ⁻¹]			[mol C:mol P]	
<i>November 2014</i>							
10 Nov	CCS	1.5	21.9	4.9	-	154	-
12 Nov	CCS	1.9	25.7	-	-	132	56
18 Nov	CS2	2.2	42.3	4.6	62	75	37
20 Nov	CS2	2.0	34.7	4.0	83	110	75
22 Nov	CCS	1.5	25.0	2.8	59	172	113
25 Nov	CCS	1.4	29.1	3.0	102	188	123
Mean		1.7	29.8	3.9	77	132	81
<i>April 2015</i>							
04 April	CCS	0.7	8.9	0.5	78	82	76
06 April	CCS	1.7	11.6	-	-	57	51
10 April	CS2	0.7	10.6	0.5	35	54	46
11 April	CCS	1.0	4.6	1.3	24	92	75
15 April	CCS	0.5	2.2	1.0	11	256	195
20 April	CCS	0.7	1.9	0.9	8	109	76
24 April	CS2	0.7	3.0	1.1	4	100	54
25 April	CCS	0.6	2.2	1.4	17	182	143
Mean		0.8	5.6	0.9	25	116	90
<i>July 2015</i>							
14 July	CCS	1.1	3.9	1.4	239	53	52
15 July	CCS	2.1	3.9	-	-	37	-
19 July	CS2	1.9	1.7	1.0	45	45	43
20 July	CS2	3.1	2.7	-	-	35	33
24 July	CCS	3.1	8.8	-	-	40	37
29 July	CCS	4.4	3.2	1.0	88	21	20
30 July	CCS	2.5	7.7	-	-	77	68
Mean		2.6	4.6	1.1	124	44	42

Poulton et al., P-dynamics, PiO Supplementary Table S1

Percentage Light Depth	LED Panels	Neutral density type (% transmission)	Measured Irradiance ($\mu\text{mol quanta m}^{-2} \text{ s}^{-1}$)	Target Photon flux ($\text{mol quanta m}^{-2} \text{ d}^{-1}$)	Actual Photon flux ($\text{mol quanta m}^{-2} \text{ d}^{-1}$)	
<i>November 2015 (photoperiod = 9 h; $E_0 = 8.7 \text{ mol quanta m}^{-2} \text{ d}^{-1}$)</i>						
60%	2	2 x 0.15 ND (69%)	167	5.2	5.4	0.60
40%	1	None	147	3.5	4.8	0.53
20%	1	0.30 ND (51%)	70	1.7	2.3	0.25
10%	1	0.15 ND (69%)	26	0.9	0.8	0.09
5%	1	0.9 ND (14%)	15	0.4	0.5	0.05
s1%	1	1.2 ND (7%)	7	0.1	0.2	0.03
<i>April 2015 (photoperiod = 14 h; $E_0 = 33.9 \text{ mol quanta m}^{-2} \text{ d}^{-1}$)</i>						
60%	3	None	440	20.3	22.2	1.58
40%	3	1 x 0.15 ND (69%)	260	13.5	13.1	0.94
20%	3	3 x 0.3 ND (51%)	120	6.8	6.0	0.43
10%	1	0.3 ND (51%)	68	3.4	3.4	0.24
5%	2	2 x 0.9 ND (14%)	21	1.7	1.1	0.08
1%	1	1.2 ND (7%)	7	0.3	0.4	0.03
<i>July 2015 (photoperiod = 16 h; $E_0 = 39.8 \text{ mol quanta m}^{-2} \text{ d}^{-1}$)</i>						
60%	3	None	440	23.9	25.3	1.58
40%	3	1 x 0.15 ND (69%)	260	15.9	15.0	0.94
20%	3	3 x 0.3 ND (51%)	120	8.0	6.9	0.43
10%	1	0.3 ND (51%)	68	4.0	3.9	0.24
5%	2	2 x 0.9 ND (14%)	21	2.0	1.2	0.08
1%	1	1.2 ND (7%)	7	0.4	0.4	0.03

FIGURES

Figure 1. Location of the sampling stations in the Celtic Sea for this study: CCS, Central Celtic Sea site; CS2, Shelf edge site.

Figure 2. Box and whisker plots of: (a) phosphate (P_i) concentration (nmol P L^{-1}); (b) chlorophyll-*a* (Chl-*a*) concentration (mg m^{-3}); (c) dissolved organic phosphorus (DOP) concentration (nmol P L^{-1}); and (d) particulate organic phosphorus (POP) concentration (nmol P L^{-1}). Plots show median (solid line), as well as the 10th, 25th, 75th and 90th percentiles.

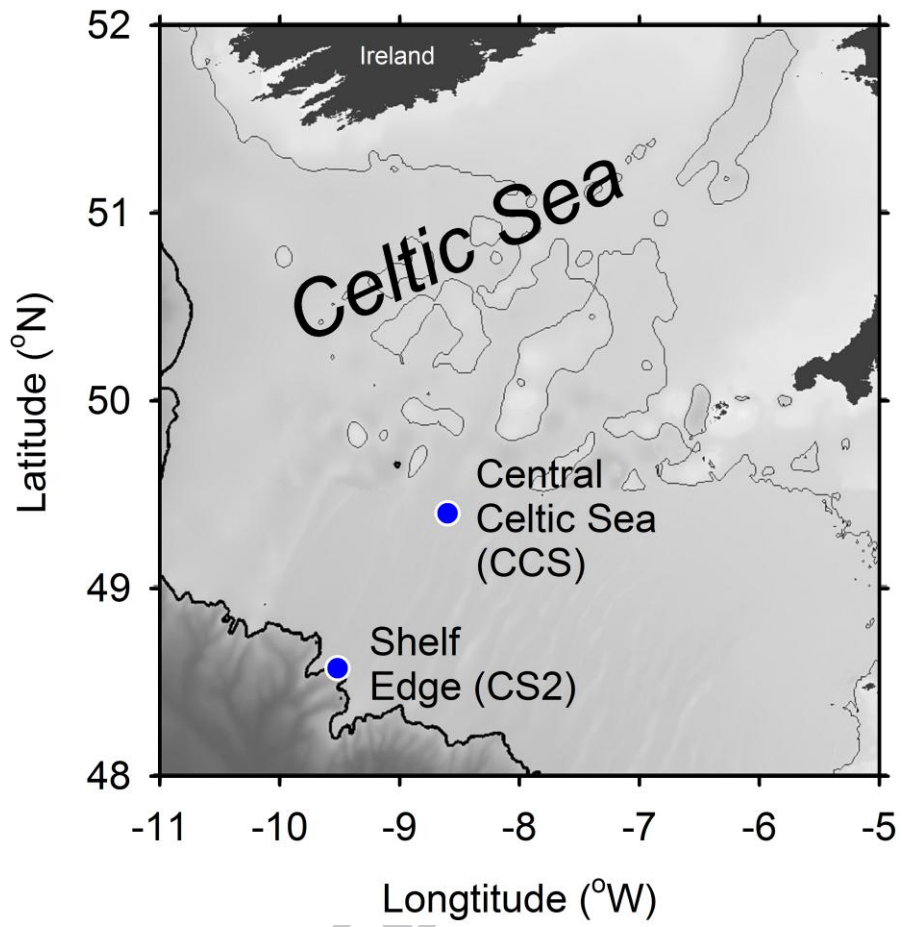
Figure 3. Box and whisker plots of: (a) phosphate (P_i) uptake ($\text{nmol P L}^{-1} \text{ h}^{-1}$); and (b) the ratio of light to dark P_i -uptake (L:D). Dashed line on (b) indicates 1:1. Plots show median (solid line), as well as the 10th, 25th, 75th and 90th percentiles.

Figure 4. Box and whisker plots of: (a) dissolved organic phosphorus (DOP) production ($\text{nmol P L}^{-1} \text{ h}^{-1}$); (b) the ratio of light to dark P_i -uptake (L:D); and (c) dissolved organic phosphorus (DOP) production expressed as a percentage of total P_i -uptake (Percentage Extracellular Release, PER). Dashed line on (b) indicates 1:1. Plots show median (solid line), as well as the 10th, 25th, 75th and 90th percentiles.

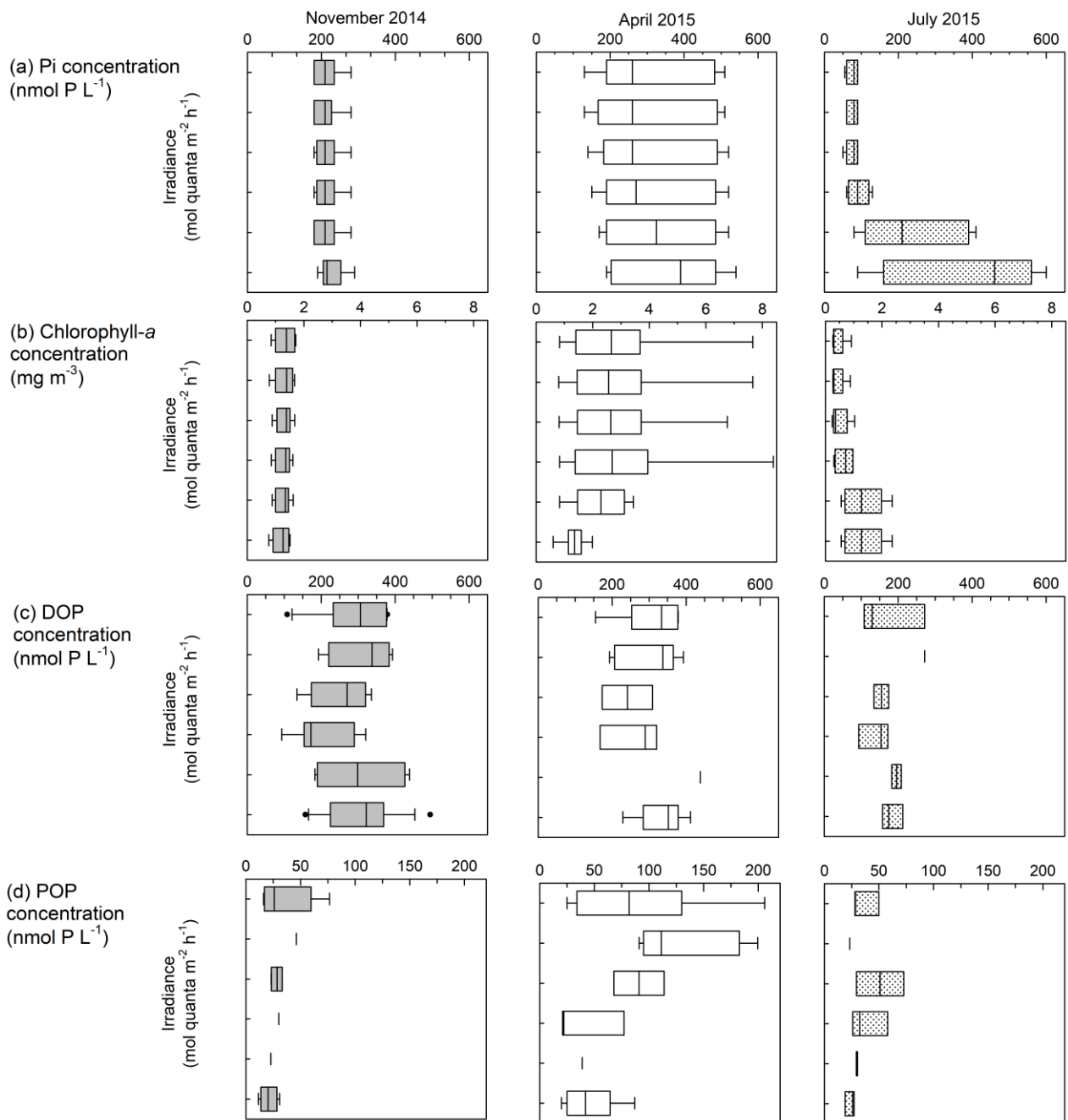
Figure 5. Time-series measurements of P_i uptake for two temporal experiments: (a) hourly P_i -uptake rates at 4 h time points over 24 h; and (b) cumulative P_i -uptake over 24 h. Dashed vertical lines indicate sunset (21:00 GMT) and sunrise (05:00 GMT). Cumulative P_i -uptake was $17.1 \text{ nmol P L}^{-1} \text{ d}^{-1}$ and $22.7 \text{ nmol P L}^{-1} \text{ d}^{-1}$, respectively.

SUPPLEMENTARY FIGURES

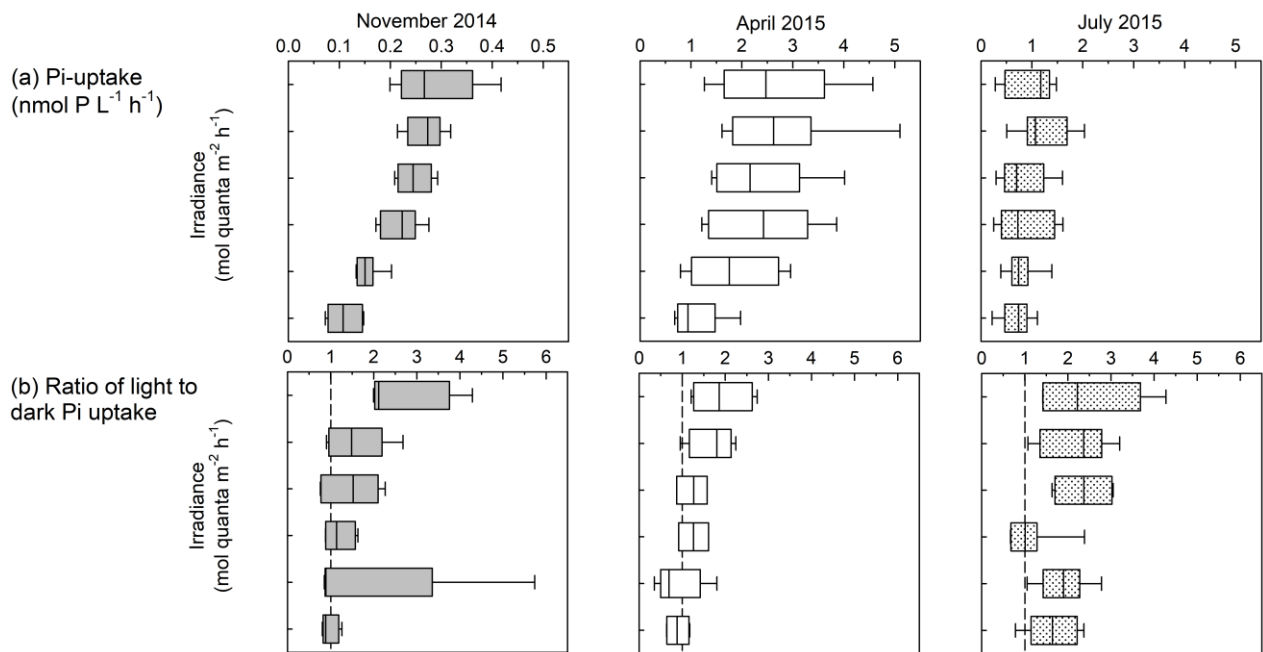
S1. Size-fractionated P_i -uptake for surface waters at three sites in the Celtic Sea.

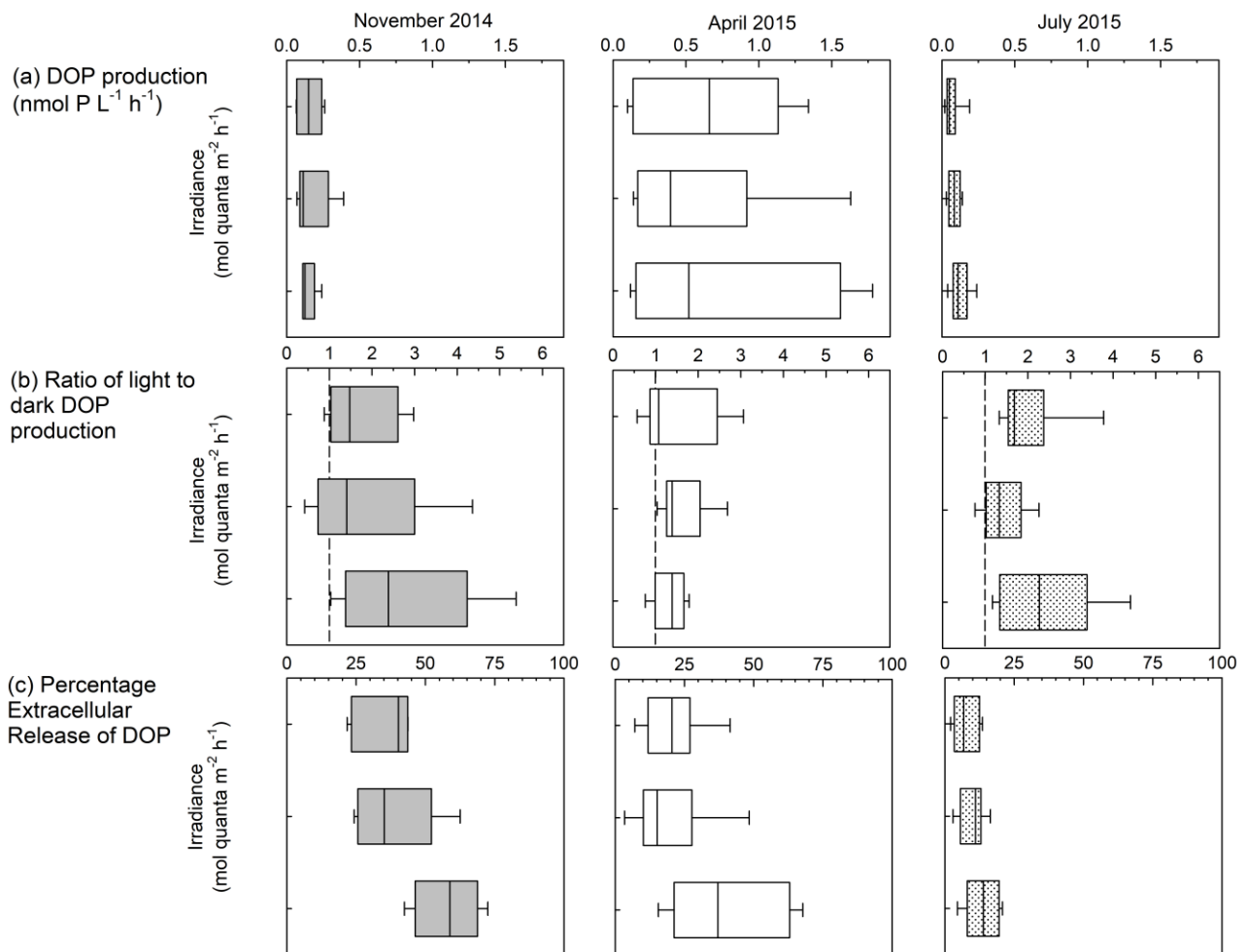


ACCEPTED

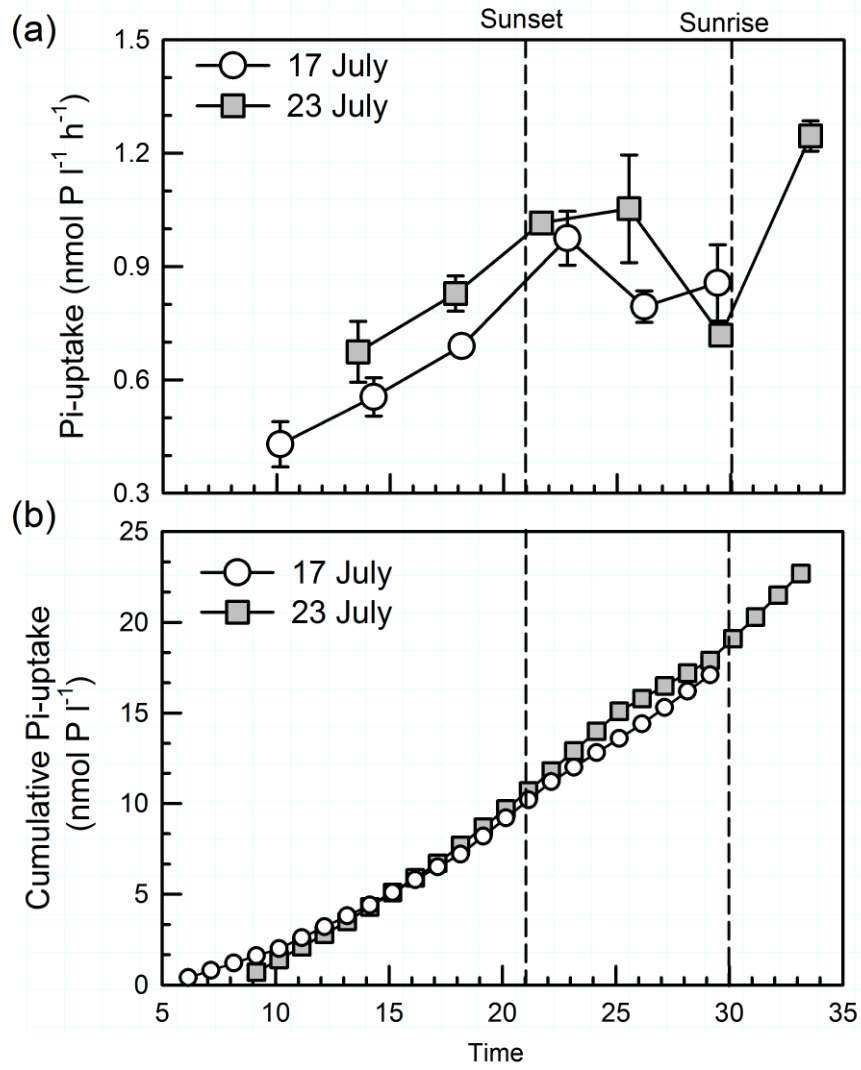


AC





ACCEPTED



SCRIPT

ACCEP